OULUN YLIOPISTO
UNIVERSITY of OULU

DEGREE PROGRAMME IN WIRELESS COMMUNICATIONS ENGINEERING

MASTER'S THESIS

FASTER THAN NYQUIST SIGNALING AND ANALYSIS OF ITS PERFORMANCE UNDER UNCODED/CODED TRANSMISSION SYSTEMS

Author	Ishwor Hadkhale
Supervisor	Prof. Nandana Rajatheva
Second Examiner	Dr. Pekka Pirinen

March, 2015

Hadkhale I. (2015) Faster than Nyquist Signaling and Analysis of its Performance Under Uncoded/Coded Transmissions Systems. University of Oulu, Department of Communications Engineering, Degree Programme in Wireless Communications Engineering. Master's Thesis, 68p.

ABSTRACT

The future demand of increased transmission rate and bandwidth efficiency is of prime concern in the modern wireless communication systems. Faster than Nyquist signaling (FTN) is under the great interest of research to address this issue of high data rate, which is also a major requirement, for the fifth generation (5G) communication networks.

The data bits are transmitted at a rate higher than the conventional methods which are bounded by the Nyquist condition and the outputs are compared so as to analyze the benefits. Receiver processing techniques are implemented to achieve the high data rate with improved error performance at the lower decoding complexity.

Considering the bandwidth efficiency as a key factor, more data symbols are sent at the given time interval by reducing the time period for signal transmission. This ensures more data being transmitted. In the scenario of perfect Nyquist signaling, pulse designs were based on the principle of orthogonality. The signal pulse form $h(t)$ is orthogonal with respect to shifts by nT, where T is the signaling interval. In the thesis, the time period is reduced to $T < 1$, which prompt more symbols to be transmitted. The pulses are no longer orthogonal. These non orthogonal FTN signals are accepted as a promising approach for the required solution of increased data rate.

FTN comes as a tradeoff between the high data rate achievement and error probability. Reduction of the time factor affirms good data rate but at the same time, cost of high error rate has to be paid. Efficient receiver processing techniques are designed to compensate between these two factors. Main obstacle due to the reduction of time period in FTN signaling is to tackle the unavoidable inter symbol interferences (ISI). Going beyond the Nyquist bound, as a consequence, results high ISI. This necessitates an effective receiver processing to overcome the ISI. Minimum mean square error (MMSE) detection algorithm is employed to equalize the received signals and analyze the performance of the FTN system.

Finally, the system portrayal is studied by processing the results under the implementation of turbo coding systems. The bit error rate (BER) characteristics are analyzed under these circumstances. Efficient encoding pattern and decoding algorithm helps in reducing the errors. Analysis of the simulation results show that the turbo code proficiency is improved by increasing the number of iterations. Performance indication is also related to the frame size or the interleaver size and the signal power. In other words, it comes as a trade-off between energy efficiency, bandwidth efficiency, complexity and error rates.

Furthermore, for the fair comparison of the performance analysis, transmission rates for turbo coded transmission systems under the conditions of Nyquist signaling and FTN signaling are made equivalent.

Keywords: Faster than Nyquist signaling, Inter symbol interferences, MMSE Equalization, Turbo coding.

CONTENTS

PREFACE

This Master's thesis is done as a part of the 5G to 10G project in the Centre for Wireless Communications, Department of Communications engineering, at the University of Oulu. The project is supported by Broad-com Communications Finland Oy, Elektrobit Wireless Communications Oy, Huawei Technologies Oy (Finland) Co. Ltd, Nokia Networks Oy and Finnish funding agency for innovation (Tekes). I would like to take the opportunity to thank all the partners funding the project and the thesis.

I would like to express my sincere gratitude to Prof. Nandana Rajatheva for providing me an opportunity to work on this thesis topic and also for his guidance and support throughout the work. I am very grateful to Dr. Fatih Bayramoglu for his meticulous support and encouragement during the thesis work. I would also like to extend my sincere appreciation to the second examiner of my thesis Dr. Pekka Pirinen for reviewing the thesis and providing me helpful advice and comments. Furthermore, I would like to thank all the members of Centre for Wireless Communications for the good working environment.

Finally, sincere thanks and appreciation goes to my family and friends for their invaluable support.

Oulu, Finland, 2015

LIST OF SYMBOLS AND ABBREVIATIONS

E_b	bit energy
$\beta_k(m)$	backward state metric
B	bandwidth
H	channel matrix
$*$	convolution operator
dB	decibel
$\delta(t)$	delta function
$G_{l,l}$	equalizer coefficient
e_l	error signal
$\alpha_k(m')$	forward state metric
$G[D]$	generator polynomial
x_π	interleaved data
$\hat{a}_{(k)}$	input sequence estimate
a_n	information sequence
λ^k	log aposteriori probability ratio
$C(z)$	mmse response in frequency domain
J_l	mean square error
N_0	noise power density
$\omega(t)$	noise signal
P_0	parity bits
$h[n]$	pulse impulse response
Λ_{d_i}	probability measure
$X_{rc}(f)$	frequency response of a raised cosine function
$G_r(f)$	frequency response of a receiver filter
R_1^k	received noisy sequence
β	roll-off factor
$y(t)$	received signal
E_s	symbol energy
f_s	sampling frequency
T_0	symbol interval for FTN
α	FTN factor
R_s	symbol rate
$s(t)$	signal response at the output of pulse shaping filter
T_s	symbol time period
σ	time delay
$G_t(f)$	frequency response of a transmitter filter
G^N	N$\times$ N toeplitz matrix
$\gamma_k^i(m', m)$	transition probability from state m' to m at stage k for input i
d_i	message bit associated with a transition in the trellis
$x[n]$	transmitted symbols
$v[n]$	upsampled signal response
σ^2	noise variance
$H(z)^{-1}$	white filter frequency response

1G	first generation
2G	second generation
3G	third generation
3GPP	3rd Generation Partnership Project
4G	fourth generation
5G	fifth generation
APP	a priori probability
AWGN	additive white Gaussian noise
BCJR	Bahl-Cocke-Jelinek-Raviv
BER	bit error rate
BPSK	binary phase-shift keying
DTFT	discrete-time Fourier transform
E-UTRA	Evolved Universal Terrestrial Radio Access
E2E	end to end
FBMC	filter bank multi carrier
FDE	frequency domain equalization
FEC	forward error correction
FFT	fast Fourier transform
FTN	faster than Nyquist
GSM	Global System for Mobile
HSPA	High Speed Packet Access
i.i.d	independent and identically distributed
ICI	inter channel interference
IoT	Internet of Things
IP	internet protocol
ISI	inter symbol interference
ITU	International Telecommunications Union
LAPPR	logarithms of a posteriori probability ratio
LDPC	low-density parity check
LLR	log-likelihood ratio
LMDS	Local Multipoint Distribution Service
LTE	Long Term Evolution
MAP	maximum a posteriori
MC-CDMA	Multi-Carrier Code Division Multiple Access
MF	matched filter
MIMO	multiple input multiple output
MMSE	minimum mean square error
MSE	mean square error
OFDM	orthogonal frequency division multiplexing
PAPR	peak to average power ratio
PAR	peak to average ratio
PHY/MAC	physical layer/ medium access control
PSD	power spectral density
QoS	quality of service
RAT	radio access technologies
RC	raised cosine
RRC	root raised cosine
RSC	recursive systematic convolutional
SISO	soft input soft output

SNR	signal to noise ratio
SOVA	soft output viterbi algorithm
UMTS	Universal Mobile Telecommunication Systems
UWB	ultra-wide band

1. INTRODUCTION

The development of fourth generation (4G) mobile communications, also known as Long-Term Evolution (LTE) or Evolved Universal Terrestrial Radio Access (E-UTRA), has been accepted as the latest solution for the user demand of faster, reliable and efficient communication systems. The latest trend in the use of these services has clearly showed the rapid increase in the demand of more promising approaches. In general, this requirement of high wireless data traffic is expected to increase dramatically by more than 500 times within 2020 as compared to present traffic [1]. Though the present technology can handle the situation for few more years, yet the large growth experienced in wireless communications has challenged the researchers to develop novel and innovative ideas more efficient than current LTE advanced technologies. The present radio access techniques thus require an adoption of more advanced technological means and the spectacular improvement.

Baseband transmission of a digital signal is expected to maintain high speed data and good quality service on the background of low-pass channel with an extremely wide bandwidth. However, the real world scenario is not always as desired because of the limited resources of the spectrum availability. Frequency band requirement is directly proportional to the signaling speed, and therefore bandwidth scarcity has become an important concern. High speed and high quality data services with an integration of variety of communicating standards are important prerequisites for future wireless communication systems. Although due to the latest developments in the technical aspect of wireless communications has helped to increase the performance out of available bandwidth spectrum, it has to be accepted with very high cost for the mobile operators to pay for the allocated spectrum resources. Limited radio spectrum provided by the regulatory organizations has complicated the task of system design to meet the very fast pace evolutional growth of communication technology. This has posed a great challenge to engineers for an efficient bandwidth management.

Energy and bandwidth usage by the transmission signals put forward a strong limitation in the world of wireless communication. The minimum bandwidth requirement for an error free transmission is defined by the Nyquist criteria [2]. Under Nyquist condition, the symbols are transmitted in different time intervals independently such that there is no inter symbol interference (ISI). This approach simplifies the task of theoretical analysis and receiver design. But the thesis work is focused to minimize the usage of the required bandwidth proposed by Nyquist and at the same time trying to minimize the interference.

The approach of using the non-orthogonal pulses for the transmission can be considered as one of the promising solutions that help to improve the efficiency of the bandwidth spectrum [1, 3–6]. Faster than Nyquist signaling (FTN) is such transmission scheme that addresses this issue by providing high data rate of transmission with the spectral efficiency. The ability of FTN transmission to achieve the higher transmission rate beyond the Nyquist criterion has gained an interest as it can provide such benefit of increased data rate within the same spectral occupancy and same bit energy consumption as that of conventional Nyquist systems.

The high speed data transmissions that can be achieved by using such non orthogonal pulses on the other hand are very likely to produce the interferences. In FTN transmission, the ISI is introduced since the signals are transmitted at a higher signaling rate than the rate forwarded by the Nyquist orthogonality criterion. For the better error performance with good bit error rate (BER), frequency-domain equalization (FDE) based on minimum mean square error criterion (MMSE) is preferred [7]. In addition, shaping of the transmitting symbols help to minimize the bandwidth consumption and eliminate the ISI between the symbols. This is explained by the pulse shaping filters.

Equalizer designing task is carried out considering the fact to overcome both the ISI and the effect of non-white noise inherent during FTN induced transmissions. The receiver input has the received signal preceded by a matched filter output. Matched filter is followed by a noise whitening filter. This whitening filter is also known as whitened matched filter [2].

Turbo coding, introduced in 1993 by Berrou, Glavieux and Thitimajshima [8], has manifested a great impact among the research communities in the field of digital communications and coding theory in the recent years. Theoretical upper bound on the channel capacity was put forward by Shannon in 1940s, for a given bandwidth, data rate and signal-to-noise ratio (SNR). However, the practical codes were not able to reach close to this theoretical bound. Finally in 1993, a new coding scheme called turbo codes were introduced which showed the possibility to achieve the capacity very close to the Shannon limit. These codes gained the wide range of applications in latest wireless standards like Universal Mobile Telecommunications System (UMTS) and LTE. These coding systems are introduced as a new class of convolutional codes. Turbo codes have the BER performance close to the Shannon limit [8]. A basic turbo encoder uses two or more component encoders concatenated in serial or parallel and separated by an interleaver. Decoding is performed iteratively to increase the reliability of the decision with some feedback decoding principles. Decoder structure deals with the coding gain achievability and the ISI mitigation. Turbo coding, with the use of the techniques like interleaving and parallel concatenation, helps to achieve high coding gain and the near optimal performance [9, 10]. The performance of the turbo code in the scenario of FTN transmission systems with ISI is also investigated in the thesis.

1.1. Thesis overview

The thesis deals with two approaches for the analysis of FTN signal transmission. At first it studies about the signal transmission for the information bits transmitted where the data bits are sent faster than the rate prescribed by Nyquist. The general approach of such system with uncoded data bits and the equalized frequency response at the receiver is studied. Second part of thesis deals with the coded data sequences. The transmission process is facilitated with the turbo coded data bits. Study of the encoder, the encoding and decoding procedures has been done for the normal Nyquist signal transmission and FTN signals. Then the comparison of these two results has been discussed.

In essence, the research work is focused to ensure the signal transmission with the maximum possible data rate and minimizing the effect of the so induced unavoidable ISI. At first the performance analysis is studied for these FTN symbols along with MMSE equalization effect. This is followed by the overall study of combining effect of the equalization techniques along with the effect of turbo coding.

The thesis is organized into seven chapters. Chapter 1 discusses an introduction about the thesis work considering general FTN signaling phenomenon and the turbo coding systems. Chapter 2 gives an overview of basic 5G networking systems and the benefits of FTN systems that directly help in meeting the few requirements of 5G systems. Chapter 3 is related to the necessary literature review and background study relevant to the entire research task. It includes an overview of the signal transmission and receiving process and also the FTN system. Also turbo codes are discussed in this chapter including the encoder and decoder architecture, the interleaver and decoding phenomenons. System model and the setup environment are explained in Chapter 4. For the performance analysis, the MATLAB implementation details and the simulation results are given in Chapter 5. This is followed by the discussion of thesis along with some future scope of the work in Chapter 6 and finally Chapter 7 concludes summarizing the thesis work.

2. 5G NETWORKS AND FASTER THAN NYQUIST SIGNALING

In this chapter, a general description about fifth generation (5G) network is discussed. In addition to this, the basic idea about faster than Nyquist (FTN) is introduced. Furthermore, the practicality of FTN signaling is presented to justify its benefit in 5G network.

2.1. Introduction to 5G Network

Wireless network refers to the communication medium between transmitter and receiver without any physical media but rather through the radio waves and micro waves. 5G network does not have specific official standardization mentioned yet. However, it is expected to have the standards much more efficient than the current standard 4G Long term evolution-Advanced (LTE-Advanced) networks. Studies and research on setting the standard for 5G are basically focused on enhancing the network in terms of bandwidth efficiency, high data rate and also the converged wireless fiber network for combining high speed and wide bandwidth feasibility [11]. It is considered as a future of mobile broadband expected to meet by 2020 [12]. Evolution in the technology of wireless communications is further targeted to the deployment of 5G network to connect the entire world more smartly with the advanced telecommunications. It is desired to improve over mobile and fixed networks with wide range of applications and varying data rates as required by the user in the multiuser environments. 5G incorporates different wireless technologies to enhance system proficiency and generate more application areas. The international telecommunications union (ITU) is extensively working to introduce the 5G with superfast, all-encompassing features along with the functioning of existing trends of 4G and third generation (3G) networks.

Cellular wireless generation has shown its evolution to next stage at around a gap of a decade starting from first generation (1G) at the beginning of 80's. From the time of 1G where it used analog signals only, with very limited facilities, the wireless network has seen a drastic improvement by the time it reached the present digital 4G network with extended multimedia services, high data rates and high quality of services (QoS). However, the future world is not satisfying with this achievement. Requirement of the technology with better coverage, low latency and extremely high reliability is increasing at very fast pace.

Previous mobile telecommunication generations like second generation (2G) were basically coverage dominated. This concept was changed to be capacity dominated by the time it reached 3G. At present, the new 4G and upcoming 5G are primarily considered as efficient energy dominated [13]. New innovations of 3rd Generation Partnership Project (3GPP) standard beyond 4G and LTE-Advanced is to be named as new generation high bandwidth and high speed internet connectivity technology. Employment of millimeter wave technologies with smart antenna structures, massive multiple input multiple Output (MIMO) concept, optimizing future PHY/MAC considerations, dense network performance improvements and cognitive radio technology are being studied aggressively to meet the 5G specifications and requirements [14, 15].

This new phase of mobile communication comes with the new network architecture consisting of user terminal and multiple independent and autonomous radio access technologies (RAT) [16]. It is an all internet protocol (IP) based model for wireless and mobile networks interoperability with adaptive new air interfaces and a common base for all radio technologies [17]. Additionally, it engulfs the feature of ultra-dense radio networking with self-backhauling, device-to-device communications, dynamic spectrum reframing and radio access infrastructure sharing [16,18]. Wireless networks with simultaneous connection to multiple wireless technologies and switching among themselves is enabled as and when required at high connectivity. Consequently, it provides the whole wireless world with complete support of multi path technology developing a complete wireless world wide web with an integrated networking.

5G network provides huge broadcasting data speed in the range of Gigabytes. It is estimated to have 1000 times higher wireless area capacity, 10 Gb/s link speed, lower end to end (E2E) latency by almost 5 times than 4G network and 90% energy saving per provided service [19]. 5G radio access will be modified considering the reference with both new RAT and evolved existing wireless technologies (LTE, High Speed Packet Access (HSPA), Global System for Mobile communication (GSM) and WiFi) [14]. The 5G mobile network supports Orthogonal frequency-division multiplexing (OFDM), Ultra-wide band (UWB) Network, Multi-Carrier Code Division Multiple Access (MCCDMA), IPv6 and Local Multipoint Distribution Service (LMDS) [14,20]. It acts as the ubiquitous mobile ultra-broadband network supporting the future internet. Current technology is providing the summed up benefit of cloud computing, more powerful terminals and high speed connectivity into a single entity as smart devices [15, 18]. Therefore, 5G network is defined to have the unified seam less environment for the integration of different wireless network technologies thereby creating substantial level of improvement in performance and capabilities over existing networks.

2.1.1. Challenges

The global race for the introduction of 5G network is expected to come up with the dramatic harmonization and improvement of the radio spectrum which creates new possibilities for the scenarios like smart cities, remote surgery, driverless cars and the new approach of internet of things (IoT). This stipulates the fact that the huge rise in the demand of connected devices is expected to grow up exceptionally. It is estimated that the demand for the inter connectivity among devices rise by 50 million to 100 million devices by 2020 [21]. In order to meet these expectations, there are many challenges to be faced, some of which in general are discussed below:

- Requirement is based on the way people use technology to communicate and access the information globally. The wireless world created by 5G network is expected to create an environment requiring very high speed applications. Achieving this high data rate is one of the major challenges.

- Dramatic increase in the traffic volume due to large number of communicating devices require the further expansion of the mobile broadband. However, the bandwidth spectrum is limited. Furthermore, in order to avoid the negative impact on mobile services, the spectrum allocation by authorities should be harmonized globally.

- The massive growth in the communication devices regarding capacity, connectivity and their diverse use compels to create a new definition to meet the requirements of future communicating devices. Assurance of efficient QoS, reliability and security is required.

- Since 5G network runs under ultra-high spectrum bands, they are more vulnerable to interferences as they travel longer distances. In addition to this, the requirement to facilitate the high speed data transmission for these densely populated user devices requires high frequency applications. This creates a great challenge to offer the wide range of coverage.

- In addition, 5G network has a challenge of maintaining desired infrastructure to meet the required specifications. Making common platform or common global standard by integrating the diverse standards is an important issue.

2.2. Faster than Nyquist Signaling (FTN) for 5G Network

5G network is a future network with an ambitious goal to achieve high speed gigabyte experience to the users with an increased capacity as compared to current LTE systems [19]. Support of the wide range of data from low rate application devices to high speed communicating multimedia devices is to be addressed. Out of the many advanced technical solutions offered in 5G networks as compared to existing networks, the unimaginably fast speed is one of the prime requirements. The network upgrade for 5G is expected to solve the requirements of most aggravating problems experienced today, i.e., the search for a fast and reliable connection. It is considered as the new wave of digital society, the emerging successor to LTE. The 5G is yet to become a standard, but the technologies under development for the network has been targeted for the situation when mobile data traffic will push the LTE networks to their limit. The proposed speed from every individual user in 5G communication system is a great challenge. This increased internet data traffic has forced for the intensive research in 5G network.

In order to make this high speed transmission achievable, various signal processing techniques like waveform coding and modulations are performed at the transmitter and receiver structures. One approach is to make the data signals travel at the rate faster than the conventional methods. Also the spectrum band has a great shortage and thus the regulatory organizations provide limited resources. So within this given spectrum, signal processing is to be done to increase the transmission speed. Use of non-orthogonal pulse symbols for the signal transmission has emerged as one of the novel solutions to address the issue [1, 6]. These non-orthogonal pulses are referred as FTN pulses where the symbol duration is reduced so as to make more data to be transmitted within the given time frame. This ensures high data rate without reducing the spectral efficiency.

Thus, in the context of the requirement of high speed communication, study of FTN comes as a promising approach. This is obtained at the cost of complex receiver structures and processing difficulties.

This thesis work, related to the use of benefits from utilizing faster than Nyquist signaling, helps to provide high speed data communication and high speed broadband wireless connection, which is one of the important parameters for the 5G networks. FTN helps the 5G network by assisting the high data rate, high channel capacity and good error rate performances.

2.3. Faster than Nyquist Signaling

2.3.1. Nyquist condition

In general, for the transmission of data over the bandwidth $(B = 1/2THz)$, we observe ISI free received signal, in the condition that it satisfies the Nyquist criteria for the orthogonal pulse shapes. The received signal in the transmission system can be expressed as

$$y(t) = \sum_{n=-\infty}^{\infty} x[n] \cdot h(t - nT_s) + \omega(t), \tag{2.1}$$

where $x[n]$, $y(t)$, $h(t)$ and $\omega(t)$ denote the transmitted symbols, received signal, impulse response (or pulse shape) and noise respectively.

Now, sampling equation (2.1) leads to

$$\begin{aligned} y(kT_s) &= \sum_{n=-\infty}^{\infty} x[n] \cdot h(k-n)T_s \\ &= \underbrace{x[k] \cdot h(0)}_{Desired} + \underbrace{\sum_{n \neq k} x[n] \cdot h(k-n)T_s\,.}_{UnwantedISI} \end{aligned} \tag{2.2}$$

The first term in the equation (2.2) represents the desired signal component while the second term represents the unwanted inter-symbol interference (ISI). In order to get rid of this ISI, the pulse response $h[n]$ must satisfy

$$h[n] = \begin{cases} 1 & n = 0 \\ 0 & n \neq 0. \end{cases} \tag{2.3}$$

Also its corresponding frequency domain representation can be written as,

$$h(t) \cdot \sum_{k=-\infty}^{\infty} \delta(t - kT_s) = \delta(t) \tag{2.4}$$

which is equivalent to equation (2.3).

Now the Fourier transformation is expressed as

$$H(f) * 1/T_s \sum_{k=-\infty}^{\infty} \delta(f - k/T_s) = 1. \tag{2.5}$$

Using the shifting property, the equation can be derived as,

$$\frac{1}{T_s} \sum_{k=-\infty}^{\infty} H(f - k/T_s) = 1. \tag{2.6}$$

This is the condition to be satisfied by the channel frequency response to ensure an ISI free transmission. Since the pulse $h(t)$ is orthogonal (Nyquist condition satisfied), the optimum detection of such signals can be performed in a symbol by symbol way using the sampler and the filter matched to $h(t)$ [6].

2.3.2. FTN Scenario

The concept of FTN as quoted by J. E. Mazo in 1975 [3] gives a motivation to study its optimal performance criteria when the signal transmission is carried out at the rate faster than the conventional rate which is satisfied by the Nyquist condition. According to Mazo, increasing the rate of transmission of the signal by 25% more than given by Nyquist rate does not degrade the minimum Euclidean distance. In other words, Mazo clarifies that for Sinc pulses, in binary signal transmission, even with the increase in the signaling speed or increasing the rate of data transmission beyond the Nyquist signaling condition, minimum Euclidean distance does not reduce much.

FTN refers to the system in which the signal is transmitted with the symbol interval $T_0 < T$, where T refers to the symbol interval for the condition which satisfies Nyquist criteria and T_0 is the new symbol interval for FTN. Reducing the symbol interval converts the Nyquist orthogonal pulses to non-orthogonal. This mechanism offers an advantage that more symbols can be transmitted in a given time frame as compared with the conventional arrangement. Thus more information can be transmitted at the rate faster than prescribed by Nyquist criteria. The equation for system with ordinary Nyquist condition

$$y(t) = \sqrt{E_s} \sum_n x[n] \cdot h(t - nT) \tag{2.7}$$

can be modified for FTN as

$$y(t) = \sqrt{E_s} \sum_n x[n] \cdot h(t - n\alpha T). \tag{2.8}$$

In the equation (2.8), $\sqrt{E_s}$ represents the symbol energy, α is the factor which determines symbol time αT (equivalent to T_0), where $\alpha < 1$.

Lower the value of α, the more will be the data rate but at the same time error rate is increased. Thus it comes as a tradeoff between these two parameters.

Unlike the ordinary linear modulation, FTN signaling system contains the pulses which are non orthogonal with respect to symbol time. The non orthogonal pulses used by FTN cause the sent symbols to be overlapped partially or fully depending upon the symbol interval T_0. This gives rise to an unavoidable ISI, which causes a degradation of the system performance. To get the benefits of FTN, these ISI needs to be eliminated. This is achieved at the cost of higher receiver complexity. Different receiver processing techniques are implemented to simplify the process.

Figure 2.1 shows the representation of the orthogonal and the nonorthogonal signals in their corresponding time domain. As seen in the Figure 2.1, with an orthogonal transmission using Sinc pulses, since the pulses are orthogonal, ensures no ISI scenario. However, in the context of non orthogonal transmission using FTN signaling, it is clear that due to the non-orthogonal pulses, time required to transmit same amount of pulse symbols is reduced as compared to previous one. But due to the non-orthogonality of the pulses, ISI is introduced.

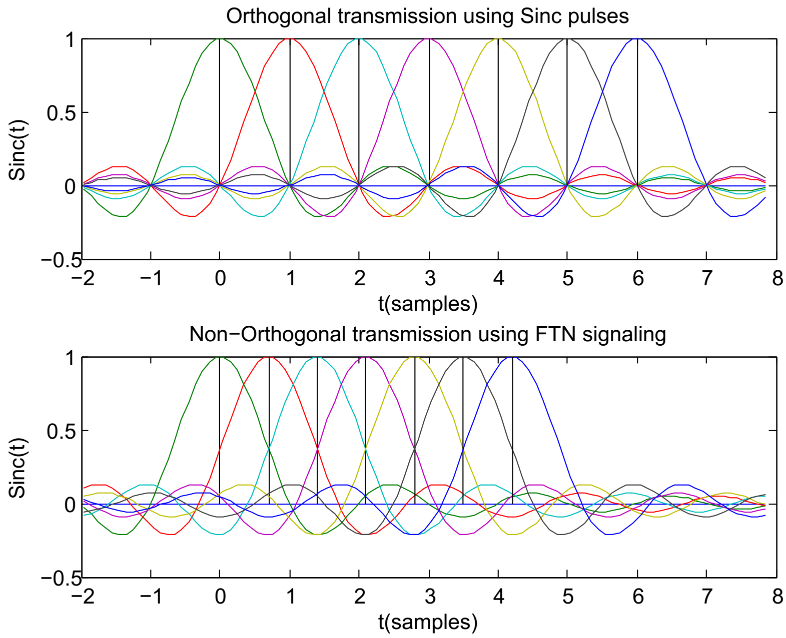

Figure 2.1: Comparision of Nyquist vs. FTN signaling in time domain.

To sum up, FTN provides a benefit of high data rate at the background of same bit energy, spectrum usage and the error rate as of orthogonal transmission systems [6]. This factor is generating interest among the researchers to address the issue of bandwidth scarcity in the modern wireless communication systems. Increasing the data rate at the same time preserving the spectral efficiency is an important benefit of FTN.

In the thesis work, study has been done to overcome the ISI that is likely to occur due to FTN. This is analyzed with the design of low complexity receiver structure.

3. LITERATURE STUDY

This chapter covers the related literature review required for the analysis of the thesis work. In general, the different terminologies and processing theories required for the understanding of signal transmission under the constraint of Nyquist criteria and FTN transmission system are presented. Theories behind the implementation of turbo coding system to analyze the coded transmission system under FTN scenario is also discussed.

3.1. Nyquist Signaling

In the study of signal processing, we define the Nyquist rate as the rate which is twice the bandwidth of a band limited signal or a channel. It can be conceptually studied relating the Nyquist rate in accordance with signaling and sampling as two different approaches.

From the sampling point of view, it is defined that in order to have no aliasing effect, the minimum sampling rate should be equal to or greater than double the highest frequency component contained within the signal. This means that sampling rate must be higher than the Nyquist rate. Sampling process involves the discretization of the continuous time signals. These samples are to be taken in a manner that it represents the original signal significantly. The number of samples taken defines the signal rate for specific signal bandwidth.

Nyquist signaling or Nyquist pulse shaping criteria highlights the necessary and sufficient condition so as to achieve zero ISI scenario. In the Nyquist paper [22], it is described about the number of pulses that could be transmitted and received over a band limited channel and also the rate of transmission. In the paper, the Nyquist signaling rate is defined as the maximum possible pulses that could be transmitted through a given bandwidth limited channel. This gives an idea about the Nyquist signaling, which provides platform for the design of the modern communication systems.

Nyquist rate clarifies the concept defining the rate as lower bound for the sample rate and upper bound for the symbol rate in a bandwidth constrained baseband channel without ISI. The upper limit for the number of bits per signal change is defined by the channel characteristics which is also known as the Shannon limit [23]. In short, the sampling frequency greater than twice the bandwidth is the condition where no aliasing effect occurs indicating the fulfillment of the Nyquist criteria. This means that for the continuous function $x(t)$ sampled at fixed sampling rate, the function that is band limited to $1/2f_s$ only satisfies the Nyquist condition, i.e., its Fourier transform

$$X(f) = 0 \quad \text{for all} \quad |f| \geq 1/2f_s. \tag{3.1}$$

For $B \leq 1/2f_s$, $2B$ and $1/2f_s$ are the expressions defining Nyquist rate and frequency respectively, where the symbol $T = 1/f_s$ represents the sample period or the sampling interval and B is the bandwidth.

3.1.1. Necessary and sufficient conditions for Nyquist criteria

In a wireless communication, when the linearly modulated symbols are transmitted, the channel impulse response or the frequency response spreads the transmitted signal in time domain. Such consecutive symbol transmission can create aliasing effect as previously transmitted signal may overlap over the other later signal. Nyquist criterion indicates the condition which when fulfilled, provides the zero ISI during such transmission.

As seen from the derivation in section 2.3, we can define the Nyquist ISI criteria as, for the discrete signals, $x[n] = x(nTs)$ and the channel impulse response $h(t) = h(nTs)$, the necessary and sufficient Nyquist condition for zero ISI or pulse shaping criteria stipulate that for a given pulse $h[n]$, it has to satisfy [2]

$$h[n] = \begin{cases} 1 & n = 0 \\ 0 & n \neq 0 \end{cases} \tag{3.2}$$

and its Fourier transform satisfy

$$\frac{1}{T_s} \sum_{k=-\infty}^{\infty} H(f + k/T_s) = 1 \tag{3.3}$$

which means that the frequency shifted versions of $H(f)$, the fourier transform of $h(t)$, is summed up to 1.

The relation (3.3) gives information that the Nyquist criterion is the condition of a wireless channel threshold for designing transceiver structures to attain an ISI free transmission. Nyquist first criterion [24] explains that the contributions at the sampling instant $(T, 2T, 3T...)$ of the received waveform must be zero. Equations (3.2) and (3.3) indicate the fact that the sum of delayed pulse spectra by k/T should sum up to T or a constant. Raised cosine pulses are such commonly used practical pulses that meet the Nyquist ISI criterion. This is discussed later in section 3.4.

3.2. Pulse shaping filters

Considering a situation for increasing data rate or transmission rate for a system with given (fixed) bandwidth without accuracy degradation, we see the bandwidth constraint to be constant. One possible way is to modify the pulses effectively such that it requires less bandwidth than the contemporary means. The pulse shape is desired to be smooth. The distorted shape may deteriorate the condition requiring larger bandwidth since such shapes contains the energy spectrum including lower frequency harmonic components. It is required that, at the perfect scenario, transmitted pulse do not interfere each other at the receiver with the successive symbols being received. The error occurred during this procedure is termed as ISI. So it is somewhat like a tradeoff between the gain and complexity. In order to have smooth shape for spectral efficiency, pulse shaping filter is selected such that it can transform the given waveform into the desired form.

The transmitted signals are the result of the data pulse passed through a pulse shaping filter which is responsible for defining the transmitter spectrum. They have a role of allocating the prescribed signal in a defined bandwidth minimizing the spectral leakage and also to maintain the high transmission rate and low error rate for a signal. In a system with band limited channels, during the increased modulation rate of a transmitted signal, it is highly probable to have distortion or the ISI due to bandwidth limitation. So it requires fixing the transmitted waveform into the shape such that signal remains in the prescribed bandwidth. Ideal filters undergo a proper sampling procedures to ensure the minimum ISI and high stop band attenuation to reduce the inter channel interference (ICI) [25].

Usually a rectangular ideal pulse is desired over an interval $[0, T]$ but the pulses having different functional forms for, e.g., Sinc pulses have the spectrum with side lobes decreasing with frequency. This causes an unintentional overlapping of the symbols from the adjacent channels or the signals. Ideally we expect the pulse with peak at $t = 0$ and zero at other sampling instants $t = T, 2T, 3T....$ In time domain it has to satisfy that its impulse response has periodic zero and zeros must occur at other sampling times, i.e., $h[nT] = 0$, where T is the data sample period. Pulses bearing such characteristics are referred as Nyquist pulses and the corresponding filters bearing such impulse responses are called Nyquist filters [26]. The pulse shaping filters are designed to satisfy the Nyquist ISI criterion.

When the band pass filtering is done prior to matched filtering, these filters reduce the cost of hardware designs as well. Pulse shaping filters implemented in frequency domain make it easy to recover the information embedded in the carrier signal by exploiting the frequency diversity at the receiver end using the signal decomposition or recombination [27].

For optimal filter design, the delta function $\delta(t)$ with pulse information is sent from the transmitter end. The full signal recovery ideal output then should be $\delta(1 + \sigma)$, where σ is the time delay of the causal system. Consequently, at the receiver end, there should be ideal output $\delta(t)$ [28].

Usually these pulse shaping filters at the transmitter is used in reference to the corresponding matched filter at the receiver unit for optimal performance. Many pulse shaping filters like Sinc shaped filter, rectangular pulse filter, Raised-cosine filter, Gaussian filter are in practice.

Here, in the thesis work, raised cosine filters are used for its best suitability satisfying Nyquist criteria and the spectral efficiency.

3.3. Roll-off factor

Roll-off factor gives the measure of the excess bandwidth occupied by any digital filter as compared to that of theoretical minimum Nyquist bandwidth. Bandwidth utilization is very important in wireless communication. In real time communication, the signals usually tend to occupy the bandwidth more than specified by Nyquist bandwidth. This excess value is referred as the roll-off factor. For, e.g., any digital filter with 100 MHz Nyquist bandwidth if occupies 130 MHz, is said to have roll-off factor 0.3 which means the filter excess bandwidth is 0.3 times the Nyquist bandwidth. It can also be defined as the steepness measure in the transition between the stop band and pass band of the filters. It directly relates to the bandwidth saving strategy. Bandwidth saving between two spectral roll-off factors can be calculated as [29]

$$Bandwidth\ saving\ (\%) = 100 - ((\beta_1/\beta_2) \times 100). \tag{3.4}$$

Here, β_1 is referred from the lower value between the two roll-off factors. Mathematically roll-off factor can be related as, for the Nyquist bandwidth of $1/2T$, if the excess bandwidth as compared to this Nyquist bandwidth be Δf, then the roll-off factor (β) is given by

$$\beta = \frac{\Delta f}{1/2T} = \frac{\Delta f}{R_s/2} = 2T\Delta f, \tag{3.5}$$

where $1/T$ is the symbol rate. The value of β lies between 0 and 1. It is an important modulation parameter to determine the signal bandwidth and spectral efficiency.

Variation in the values of roll-off factor causes a change in the characteristics of modulated signal which directly affects the impact of the transmission signal. Higher roll-off means low ISI, since it reduces the change rate of the amplitude of output pulse at zero crossings. But it makes the signal bandwidth wider consequently consuming larger spectrum. On the other hand, lower the value of roll-off factors designed, higher is the spectral efficiency achieved. However, the rate of signal decay is slowest in the time domain. This makes the baseband signal more complex. In short, comparative lower roll-off values means a corresponding decrease in bandwidth usage and increase in symbol rate and overall throughput. This highlights that the proper selection of roll-off factor plays an important role on the performance of the system designed.

The maximum symbol rate R_s attainable as studied in [30] can be related from roll-off factor for the given bandwidth as

$$R_s = B(1 + \beta), \tag{3.6}$$

where B is the bandwidth of the system and β be the roll-off factor.

3.4. Raised cosine pulse

Raised cosine (RC) filters are known for their ability to reduce the inter symbol interference of the signal. In communication systems, they are used as pulse shaping filters to shape the pulses. Basically the name raised cosine stands for non-zero portion of the frequency spectrum with roll-off factor equal to 1 which defines the cosine function raised above the horizontal axis. It is the representation of pulse spectrum. For the channel with bandwidth B, if $T > 1/2B$ then the pulse spectrum for this condition is called the raised cosine spectrum where $1/T$ is the sampling rate of the signal.

Raised cosine pulse shaping modulation is bandwidth efficient, i.e., more bits/sec/Hz and also power efficient, i.e., it requires comparatively low E_b/N_0 for same bit error rate. These pulses stand as a balance between the rectangular pulse and the Sinc pulses. Rectangular pulses have sharp edges in the time domain indicating the large bandwidth in the frequency domain. So it requires infinite bandwidth. On the other hand, Sinc pulses have an infinite length of time domain sequence. Raised cosine pulses are therefore preferred as they exhibit the balanced nature between these two pulses. These pulses do not show such infinite long nature in both the time and frequency domains. When the passband frequency of these filters is half the data rate, it satisfies the Nyquist criterion such that $T = NT_s$ [31], where T is the data period and N is any integer.

Frequency response characteristic of a raised cosine function is given by [2]

$$X_{rc}(f) = \begin{cases} T & for \quad 0 \leq |f| \leq \frac{1-\beta}{2T} \\ \frac{T}{2}\{1+\cos(\pi T/\beta(|f| - \frac{1-\beta}{2T}))\} & for \quad \frac{1-\beta}{2T} \leq |f| \leq \frac{1+\beta}{2T} \\ 0 & for \quad |f| > \frac{1+\beta}{2T}. \end{cases} \tag{3.7}$$

In the relation (3.7), β is the roll-off factor and T is the reciprocal of symbol rate. Impulse response of the spectrum for raised cosine function is given by [2]

$$\begin{aligned} x(t) &= \frac{sin(\pi t/T)}{\pi t/T} \frac{cos(\pi \beta t/T)}{1-4\beta^2 t^2/T^2} \\ &= Sinc(\pi t/T) \frac{cos(\pi \beta t/T)}{1-4\beta^2 t^2/T^2}. \end{aligned} \tag{3.8}$$

As seen in the equation (3.8), the raised cosine pulse takes the form of a Sinc pulse shapes. The bandwidth of the pulse and the rate of decay are determined by the value of roll-off factor (β). Lower the value of β, sharper the spectrum . With roll-off value 1, it gives the pure raised cosine spectrum removing the flat portion. The tails of the signal $x(t)$ is decayed as $1/t^3$ for roll-off factor greater than zero. This is the reason behind the formation of ISI which is formed when the timing mismatch occurs during sampling. Since the impulse response of RC filters has indefinite structure, it needs to be truncated for practical applications. In frequency domain, this truncation yields a non zero side lobe. However, since pulse response delay is proportional to $1/t^3$, the result might vary from that of theoretical approach [26].

Ideal response of a raised cosine filter has a unity gain in the region of low frequency and total attenuation at the high frequency. In the middle of these two frequencies, responses has a raised cosine function, size of which is determined by the roll-off factor. So they are also called low pass filters. This raised cosine function meets the requirement of a pulse shaping filter, i.e., low pass response in frequency domain, zero ISI case and finite extent in time domain [26].

For an ideal channel,

$$X_{rc}(f) = G_t(f)G_r(f), \tag{3.9}$$

where $G_t(f)$ and $G_r(f)$ are the frequency responses of the transmitter filter and receiver filter respectively [2]. These filters are used to analyze the overall desired frequency response.

For the matched condition of transmitter and receiver filter, $G_t(f) = G_r^*(f)$ which yields,

$$G_t(f) = \sqrt{|X_{rc}(f)|}e^{-j2\pi f t_0}. \tag{3.10}$$

Here, t_0 is the nominal delay that is introduced to ensure the physical realizability of the filter [2].

The ISI free nature of raised cosine filter is the main reason behind its wide use in communication systems [32]. Using these filters, matched filtering is performed

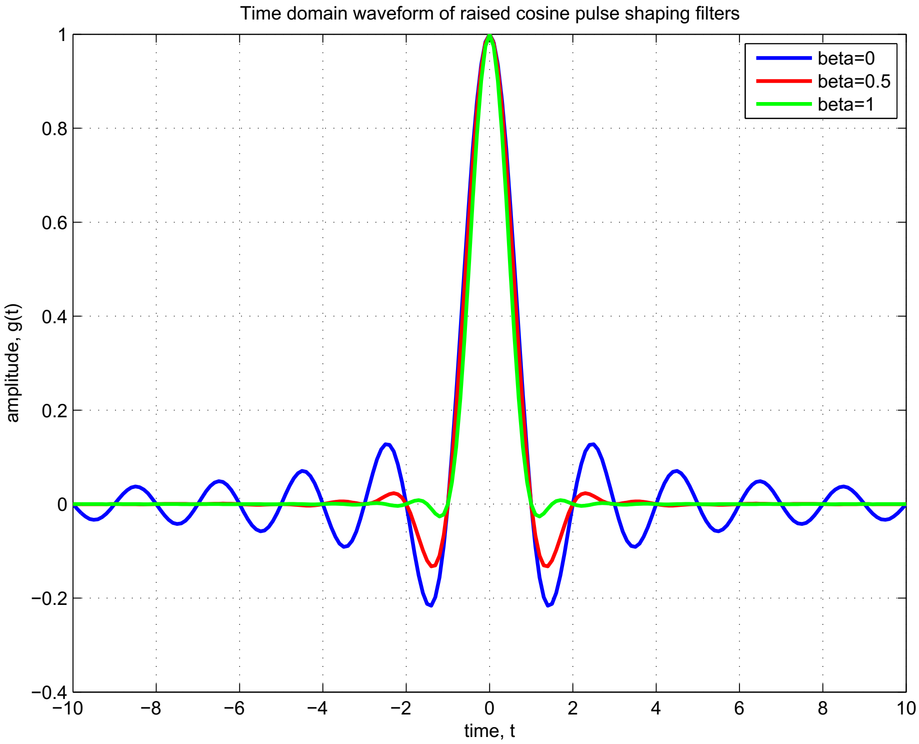

Figure 3.1: Time domain representation of Raised Cosine Pulse.

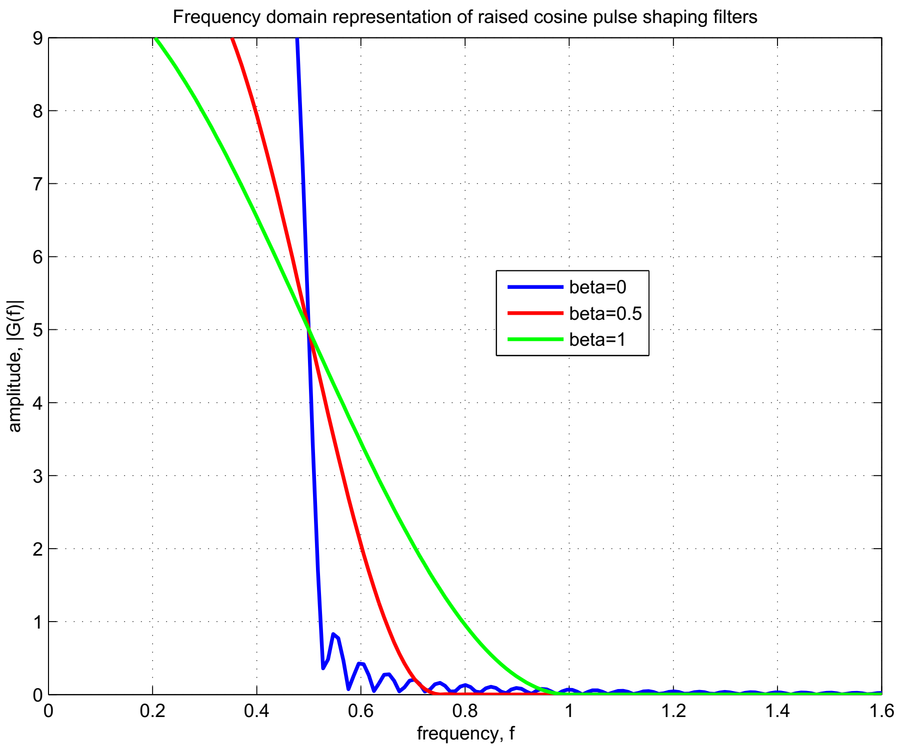

Figure 3.2: Frequency domain representation of Raised Cosine Pulse.

in the receiver to reduce the error in the received signal. Matched filter in this case reduces the noise by creating a low pass filter and also helps in ISI reduction, which is discussed more in section 3.5.

Currently the new families of raised cosine filters are under research which not only provide zero ISI but also help to decrease the peak-to-average ratio (PAR) of the baseband signal over the conventional ones [33]. The time and frequency domain representations of raised cosine pulses are shown in Figures 3.1 and 3.2, respectively.

3.4.1. Root raised cosine pulse

Like the raised cosine, root raised cosine (RRC) also called as square root raised cosine are the pulse shaping filters that help to reduce the ISI. Basically, they are the square root of the frequency response of raised cosine functions. For an ISI free transmission, the response of transmit filter, receive filter and the channel has to satisfy the Nyquist ISI criteria. Designing the matched, transmitter and the receiver filter such that their combination satisfy the Nyquist condition is an important task in defining wireless communication systems. The RRC pulse do not have the perfect orthogonal pulses, i.e., the impulse response is not equal to zero at every symbol time interval $T, 2T, ...$ and so on. However, the combined effect of these RRC pulses at the transmitter and receiver shows the characteristics of Nyquist filter thereby helping to minimize the ISI.

In a practical approach, the root raised cosine filter is used at the transmitter as a pulse shaping filter and also at the receiver as a matched filter. When a signal passes through these two identical filters, the effects of those filters are squared. This ultimately provides the total effect of raised cosine filter with an additional benefit of noise filtering at the receiver [34].

Frequency response and impulse response of an RRC pulse are given by the equations (3.11) and (3.12), respectively [31]

$$F(\omega) = \begin{cases} 1 & , \quad \omega < \omega_c(1-\beta) \\ 0 & , \quad \omega > \omega_c(1+\beta) \\ \sqrt{\frac{1+\cos(\frac{\pi(\omega-\omega_c(1-\beta))}{2\beta\omega_c})}{2}} & , \quad \omega_c(1-\beta) < \omega < \omega_c(1+\beta), \end{cases} \tag{3.11}$$

$$h(t) = \frac{4\beta}{\pi\sqrt{T}} \frac{\cos\frac{(1+\beta)\pi t}{T} + \frac{T}{4\beta t}\sin\frac{(1-\beta)\pi t}{T}}{1-(4\beta t/T)^2}. \tag{3.12}$$

The RRC filters provide a practical means for eliminating the side lobes of a spectrum. This is beneficial for the signal transmission as it has to work on a limited bandwidth. For the practical implementations, i.e., to make the filter causal, some delay is added to the pulse. Since the RRC pulses are non-causal, they are truncated so as to make them physically realizable.

Filtering is required both at the transmitter as well as at the receiver end. The noise and the interferences at the receiving side are filtered out by the receiver filter. The filter effect is viewed as the combined effects of these two transmit and receive filters. Both of these filters should abide by Nyquist criteria. The combined result due to these two filters is expressed as in the equation (3.9) as

$$X_{rc}(f) = G_t(f)G_r(f),$$

where $G_t(f)$ and $G_r(f)$ are the transfer function of the transmitter filter and receiver filter, respectively, in frequency domain. Ignoring the effect of frequency domain transfer function due to channel and assuming that the transmit filter is equivalent to receive filter, since $G_t(f) = G_r(f)$ the combined effect is therefore given by

$$X_{rc}(f) = G_t(f)G_r(f) = |G_t(f)|^2. \tag{3.13}$$

Considering this, the transfer function for the filter at transmitter side can be reduced as the square root of the transfer function due to the combined effect. The transfer function of transmitter is the square root of the raised cosine function [35]. The time domain and frequency domain representation of RRC pulse is shown in Figures 3.3 and 3.4, respectively.

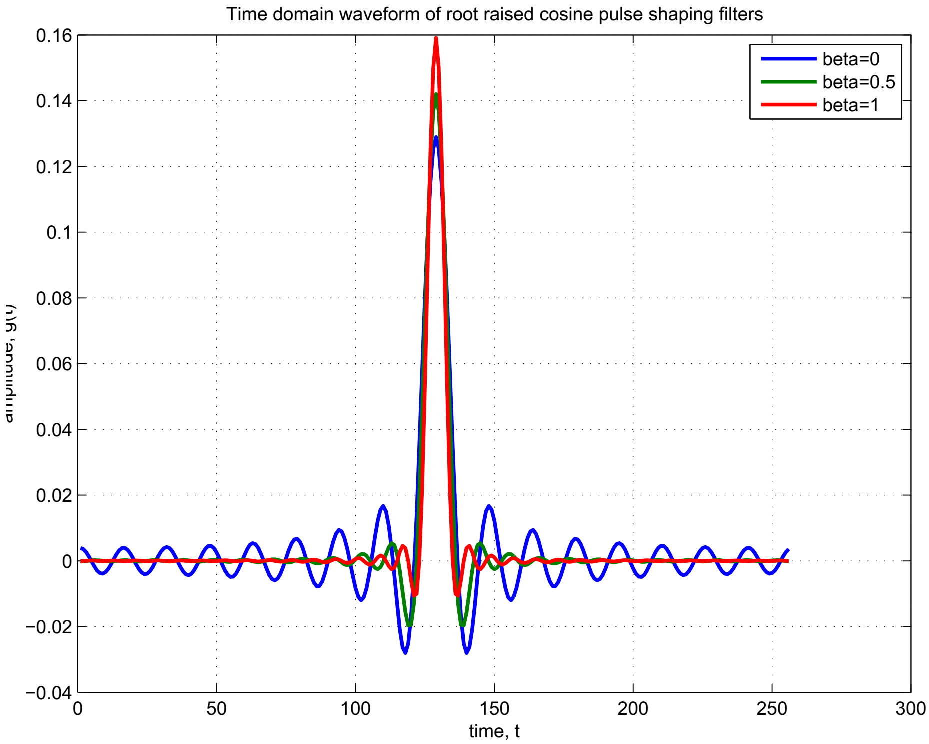

Figure 3.3: Time domain representation of RRC pulse.

The overall response of the Nyquist filter is therefore a combined effect of transmitter and receiver filter. The phase response of transmitter is compensated by receiver such that the final phase response is linear, as follows

$$\begin{aligned} X_{rc}(f) &= G_t(f)G_r(f) = |G_t(f)|^2 \\ |G_t(f)| &= |G_r(f)| = \sqrt{|X_{rc}(f)|} \\ \angle G_r(f) &= -2\pi f \tau_0 - \angle G_t(f). \end{aligned} \tag{3.14}$$

The transmit and receive filters have the linear phase with a nominal delay of $\tau_0/2$ which make the filters physically realizable [36].

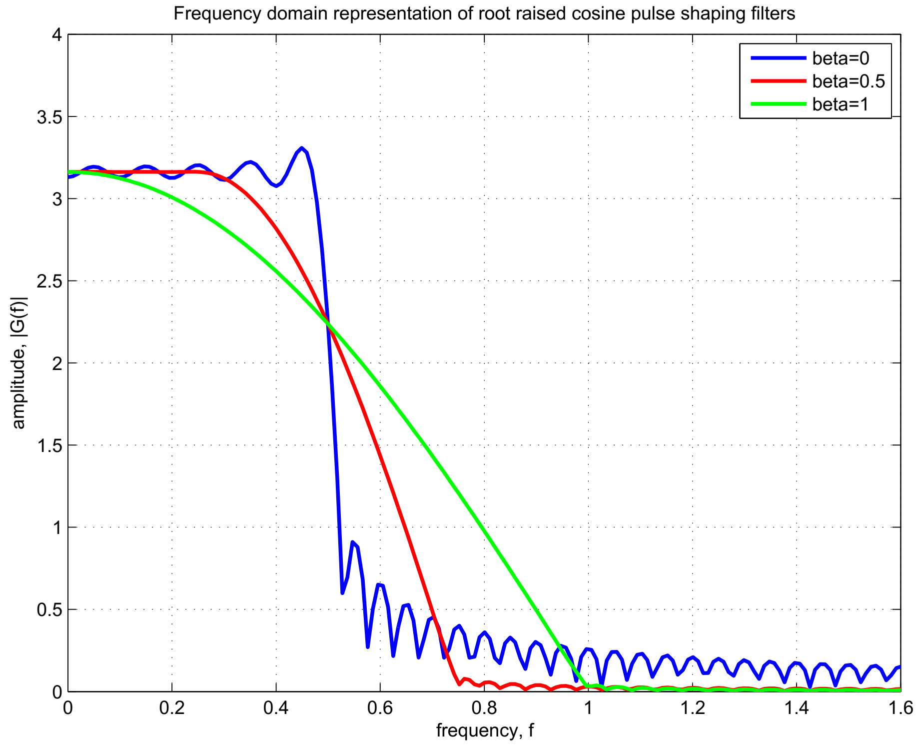

Figure 3.4: Frequency domain representation of RRC Pulse.

3.5. Matched Filters

Matched filters are the optimum linear filters used for enhancing the signal power or SNR. Basically these filters are implemented using a known signal as a reference signal and comparing the unknown signal with the known referenced signal. This is done by taking the convolution of unknown signal with the time reversed form of referenced known signal. It can also be referred as convolution of unknown signal with conjugated time reversed version of known signal. The pulse compression where impulse response is matched to input signals, radar signaling are the examples of matched filtering. They are the linear time invariant filters that increases the SNR and decreases the error probability.

Since the main principles for matched filter were developed by Dwight North in 1943, reproduced in 1963 by Lamontblake, it is also known as the North filter or conjugate filter [37]. Matched filter has its unique feature that it gives maximum possible instantaneous SNR at the output for the input of signal plus additive white noise.

The received signal consists of the transmitted pulses distorted by an additive channel noise. These noises are usually considered as additive Gaussian white noise. These received noisy signals are to be filtered out to receive the original transmitted pulse without noise components. Minimizing the noise effect out of the received signal is done in an optimum manner. Output signal power is desired to be considerably higher than the instantaneous noise power which is defined as maximizing the signal to noise power ratio. These filters give sharp peak response to the desired pulse at its input. This peak helps to determine the location t_0 and the amplitude of the pulse from received signal. The general matched filter representation is shown in Figure 3.5.

For a transmitted signal $x(t)$ and noise $n(t)$,

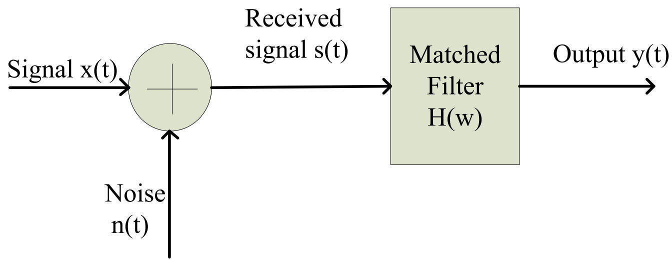

Figure 3.5: Basic representation of a matched filter.

$$
\begin{aligned}
s(t) &= x(t) + n(t) \\
\text{filter output,} \quad y(t) &= s(t) * h(t).
\end{aligned} \tag{3.15}
$$

Since the filter is linear, output can be written as,

$$
\begin{aligned}
y(t) &= x(t) * h(t) + n(t) * h(t) \\
&= x_0(t) + n_0(t).
\end{aligned} \tag{3.16}
$$

Now the matched filter is the linear filter $h(t)$ or equivalently $H(\omega)$ that maximizes the SNR.

Let the input signal for matched filter be represented by

$$x(t) = Cs_i(t - t_1) + n_i(t), \tag{3.17}$$

where t_1 is the unknown time delay, $n_i(t)$ is the input white noise and C is any constant value.

Now for the white input noise, its autocorrelation and power spectral density (PSD) functions can be written as

$$
\begin{aligned}
Rn_i(t) &= \frac{N_0}{2}\delta(t) \\
Sn_i(\omega) &= N_0/2,
\end{aligned} \tag{3.18}
$$

where N_0 is a constant value. Output can then be written as, [38]

$$
\begin{aligned}
y(t) &= Cs_o(t - t_1) + n_o(t) \\
s_o(t) &= s_i(t) * h(t) \\
n_o(t) &= n_i(t) * h(t).
\end{aligned} \tag{3.19}
$$

Here $h(t)$ is the impulse response and * denotes convolution operation.

SNR of the matched filter depends on the ratio of signal energy to the PSD of the white noise at filter output. The signal component with maximum energy occurs at the sampling instant $t = T$. In matched filter, output is proportional to the shifted version of the auto correlation function of input signal [39].

Matched filters are used considering the noise as white noise. However, if the noise is colored, the problem is solved by using the filter, known as whitening filter, which filters the input signal noise to make it white.

Matched filters are the optimal equalizers used to maximize the SNR at each beam former output beam when the impulse response is known and the noise is additive white noise. Since each different signal requires different filters, it is called matched filtering as it has to match all the waveforms. These filters, however, do not play role in minimizing ISI. Since the optimization procedure in matched filter assumes only one signal transmitted over a channel, it does not focus much with ISI [40]. It enhances the SNR by improving the received signal and not the noise.

3.6. Whitening filters

In any communication systems, noise is always an unavoidable parameter, which is present in the received signal that deteriorates the quality of signal power. Since it degrades the throughput of the system, it needs to be minimized. White noises are the ones with flat power spectrum having constant power at all the frequencies, i.e., they are random signal with constant power spectral density. They can also be considered as a sequence of serially uncorrelated random variables having zero mean and constant variance. Unlike this, colored noise is the one with varying power spectrum. Such noises increase inefficiency of the system. So it is imperative to whiten the colored noise. The filters that implement this process of whitening the noises are called whitening filters.

Whitening transformation is basically inferred as the decorrelation transformation of random variables with known covariance matrix into new set of random variables with identity matrix as its new covariance. This transforms the noise vector into a white noise vector, hence the name whitening filter. They are uncorrelated and have the variance equal to unity. Whitening filters can help minimize the interference due to other users in spread spectrum communication systems. The process is also known as digital whitening. During whitening, first the interfering signals are estimated and then the coefficients to be used in transversal filter are computed which is then followed by the filtering procedures for the received signal. In Figure 3.6, $r(t)$ is the received signal

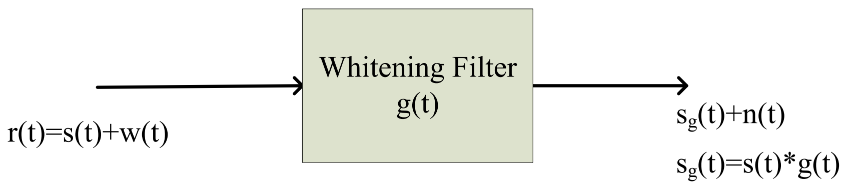

Figure 3.6: Basic flow for Whitening Filter.

comprising of signal $s(t)$ with colored noise $w(t)$, is passed through a whitening filter to get the whitened output signal. The term $g(t)$ indicates the whitening filter and $n(t)$ is the white noise having unit spectral density.

These filters can also be considered as an inverse of the system that distorts it. If the frequency response of the system is $H(Z)$, then the white filter response is $1/H(Z)$. In whitened matched filter model, noise whitening filter is introduced after the sampled matched filter. To be useful in practice, the whitening filter should be stable and causal as well.

If the filter $g(t)$ is used to whiten the noise in order to produce the output noise having power spectral density $S_n^0(f) = N_0/2$, then the filter should have [41]

$$\begin{aligned} & S_n(f)|G(f)|^2 = N_0/2 \\ i.e. \qquad & |G(f)|^2 = N_0/2 \cdot 1/S_n(f), \end{aligned} \tag{3.20}$$

where $g(t)$ is the impulse response of filter, $G(f)$ is its transfer function which change the power spectral density $S_n(f)$ of the Gaussian noise process with noise $N(t)$.

3.7. Equalizers

Wireless communications is very likely to face different frequency dependant phase and amplitude distortions due to multipath signal transmissions and fading. In signal transmission, the received pulses come in a distorted form than the original transmitted pulse. The transmission characteristics of a band limited channel or channel noise gives rise to an ISI which is the cause for the distortion of the signals. Design of the inverse filter to counterfeit the channel impulse response so as to compensate the error and retain the signals as a replica of original signal is the main task of an equalizer.

Usually the signals are given a pattern through a pulse shaping filter. Proper sampling of the signals with no addition of the noise yields no ISI scenario. However, if it is not sampled at the sampling interval or against the Nyquist condition, the signal reconstruction is not exact. Moreover, the addition of channel noise causes a distortion in signal regenerating process at the receiver. To overcome this situation, the distorted signal is passed through a filter which is basically a multiplicative inverse in spectral domain of the frequency response of a channel. This is called equalization. Thus the equalized output is considered as reliable output.

Generally for short range transmissions, preset equalizers are used since in such case channel characteristics is not an important factor that needs to be considered. This is because the channel parameters are more or less time invariant. For the long range communications, the equalizers must be adaptive such that equalizers adapt to the time varying characteristics of the channel. The equalizer adjustment algorithms are mainly based on either peak distortion criteria or mean square distortion criteria [42].

In a communication system, considered linear time invariant, output signal can be modeled as

$$x[n] = \sum_{k=-\infty}^{\infty} h[k]s(n-k) + v(n), \tag{3.21}$$

where $s[n]$ is the transmitted symbol, $h[k]$ the impulse response and $v[n]$ is additive white gaussian noise (AWGN). Now equation can be simplified as,

$$x[n] = h[0] + s[n] + \sum_{k=-\infty, k\neq 0}^{\infty} h[k]s(n-k) + v(n). \tag{3.22}$$

In equation (3.22), the second part of the equation refers to the delayed version of the transmitted symbols, which are known as inter symbol interferences. The equalizer is focused to eliminate this ISI to the minimum level possible.

Various equalization methods are implemented as demanded by the situation of signal transmitting and receiving procedures. In the thesis work, MMSE equalization method is effectuated.

3.7.1. MMSE equalization

In digital communications, equalizers come along with matched filters where equalizers are responsible to minimize ISI and the matched filters reduce the channel noise. Equalizers can be classified based on their structure, algorithms used to adapt the coefficients or their optimization criteria. MMSE algorithm makes use of the joint minimization of noise and ISI parameters.

MMSE equalization is considered as a measure of estimator quality. It is based on MMSE filtering. The linear filter which is designed to minimize the error between the transmitted signal and the received output such that original signal can be estimated out of it are the MMSE filters. The error consists of an ISI in addition to the noise. The MMSE criterion ensures an optimum tradeoff between the residual ISI in the received signal and noise enhancement. In such equalization, since the minimization of mean square error (MSE) is done, the noise amplification is reduced. This is why it outperforms the zero forcing equalizers.

The main objective of the MMSE equalizer is to minimize the variance of the error signal or the the mean square value of the error. The error signal is calculated by the help of estimated signals. It is the difference of transmitted signal and the estimate of the received signal. At low to moderate SNR values, these equalizers give remarkably lower bit errors as compared to zero forcing equalizers

$$\begin{aligned} e_l &= s_l - G_{l,l}\hat{R}_l \\ J_l &= E|e|^2. \end{aligned} \tag{3.23}$$

In the relation (3.23), J_l is mean square error, $G_{l,l}$ is equalizer coefficient, s_l is the transmitted signal, $\hat{R}_l$ the estimate of received signal and e_l is the error. Minimizing the mean square error can be done using the orthogonality principle which states that mean square error J_l is minimum if the equalizer coefficient $G_{l,l}$ is selected in a way that received signal R_l and error e_l are orthogonal to each other [43]

$$\mathbb{E}[e_l R_l^*] = 0. \tag{3.24}$$

Now the equalizer coefficient for the MMSE equalization is calculated by the equation

$$G_{l,l} = \frac{H_{l,l}^*}{|H_{l,l}|^2 + \sigma^2} \ , \tag{3.25}$$

where H represents the channel matrix with the diagonal components $H_{l,l}$ and σ^2 represents the noise variance.

Equation (3.25) infers that MMSE computation needs the value of noise variance (σ^2), which is determined during the system design that helps MMSE equalizer give the optimal performance.

3.8. Turbo coding

Coding basically refers to the mechanism where information sequences are encoded in a manner such that when transmitted over noisy channel, still retains the original signal at the decoder when decoded. Usually coding is viewed as the source coding and channel coding. Source coding refers to the modification of message source to the code in the form that could be transmitted through channel. Channel coding means the encoding of the message that results from source coding such that by introducing some form of redundancy, error correction and message detection is done reliably at the receiver.

Turbo codes from the time of its introduction [44, 45] are gaining interest in the research field and investigation of coding theory as a new approach to error correction code. This is due to its high coding gain and near Shannon capacity performance.

Turbo codes are the derivation of convolution codes, class of high performance forward error correction (FEC) codes. These convolution error correcting codes use a soft iterative decoding procedures resulting in the high coding gains than the conventional convolution codes. They offer a wide range of wireless communication applications applicable from 3G mobile systems to deep space explorations. Turbo codes are used extensively in modern wireless communication systems like LTE and LTE-A. Basically, it consists of recursive systematic convolution (RSC) encoder, interleaver and an iterative decoder. Using an iterative a posteriori probability (APP) decoder was introduced which provided low BER at the SNR very close to Shannon theoretical limit [45]. Maximum a posteriori (MAP) algorithm was used for the coded sequences by Bahl Cocke Jelinek Raviv (BCJR) [46]. These error correction codes are widely used in the field areas which expect a good power saving scenario and low SNR requirement. Parallel concatenated turbo codes, serial concatenated turbo codes, and repeat-accumulate codes are some of the examples of turbo code implementation.

During coding, the information bits are mapped to the code bits. This is done by convolving the information bits with the generator sequence code bits. Turbo codes are preferred over the other FEC codes as they provide better result compared to others at least by 3 dB, saving approximately 20% of bandwidth spectrum [47].

Code rate is used to explain the redundancy of the code. Turbo codes used in the thesis are the parallel concatenated convolution codes with rate k/n, where k and n denotes the information bit sequence in the encoder and output bits, respectively. Check sequences transmitted together, also called as parity bits, is represented by *n-k*. Lower rate refers to more redundancy. Lower rate codes, since can correct more errors, come with the benefit of low transmit power, large transmission distance and high data rate. But this comes at the cost of large bandwidth consumption. In addition, decoding complexity is exponential to the code size. So these long size low rate codes have high computational complexity. It is considered as a tradeoff between the bandwidth and energy efficiency. For a given transmission rate, noise power and bandwidth, there exists fixed lower bound for the bit energy. Shannon capacity is fixed for the given bit with code energy efficiency [48]. Different rates for turbo codes can be produced by puncturing the parity bits [49]. Basic structure for the coding system is shown in the

Figure 3.7.

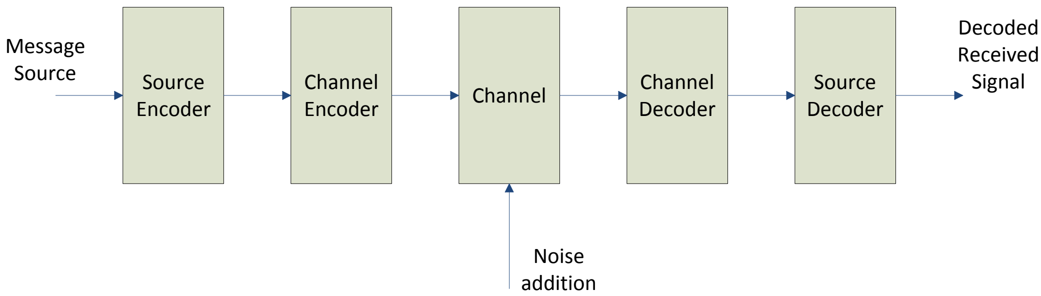

Figure 3.7: General representation of basic coding structure.

3.8.1. Encoder

Encoders in the turbo code consists of a serial or parallel RSC encoders. In the thesis work, parallel concatenation is implemented as it performs better than the serial concatenations [50]. These parallel concatenation of RSC encoders are separated by an interleaver, denoted by π. The basic encoder structure is shown in the Figure 3.8.

The transmitted signal k and the interleaved version of the same are transmitted through it. At the input of the second encoder the non uniform interleaver scrambles the regular order of the data bits. In the thesis work, pseudo random interleaving pattern is used. The code rate can be increased using some puncturing techniques which enable selecting the pattern of the coded bits. Thus the encoders are coding the same information sequence but in different order. Consequently, output of second encoder will obviously be different than the first one.

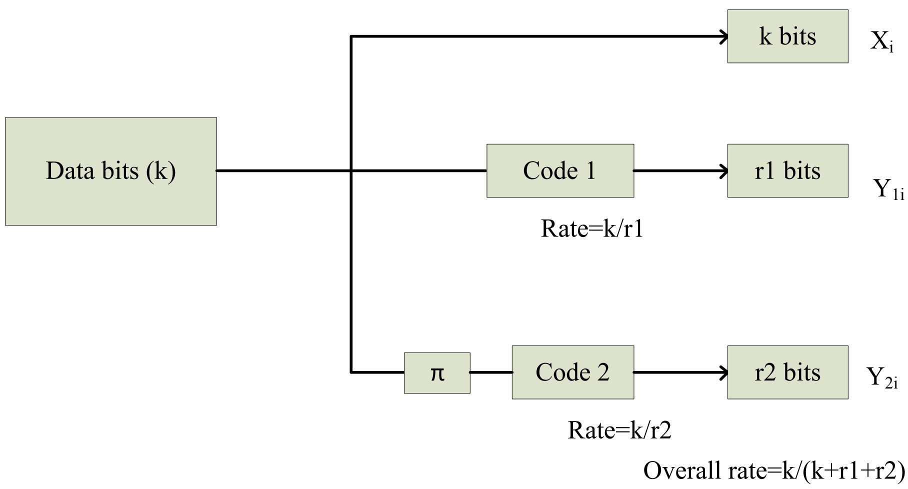

Figure 3.8: Basic encoder structure [48].

The interleavers used are identical. These interleavers help to compensate for the possible errors bursts that might occur due to decoder imperfection. First the code is in systematic order. The code through interleaver faces the bits in some random pattern depending upon the type of the interleaver used such that the bits are scrambled. Interleaver selection is therefore considered as an important task [49, 51]. The output of one encoder is different from the other which means it has two different output weights. If one of the outputs is lower, then high weight can be expected from the next. Higher weight words are better for the decoder. The pseudo random bitwise interleaving between the encoders help to improve the system performance reducing the bit error. Turbo produce high weight codes. Usually the coder size is kept low, typically two, since the increase in its size is not justified in the sense of performance vs. complexity and overhead. Two encoders have time displaced codes from same input sequence. These two coded output from the first and the interleaved one are multiplexed to refer the code rate. Interleaver at the encoder produces lower weight sequences at the output of first transmission such that during the retransmission output weight sequence is higher. These two transmissions and retransmitted sequences are combined at the receiver.

The interleavers at encoder and iterations at decoder might cause comparatively high latency and higher decoding complexity. With the increase in the size of interleaver, decoder latency also increases [52]. But it comes as a tradeoff between the complexity and better performance. For every channel, it is associated with channel capacity c, which is an upper bound with information rate r. The efficient and reliable communication is guaranteed with rate $r < c$. The bit error probability decreases as the block length n of the code increases, with the rate given $r < c$ at random. As explained by Shannon, increment in randomness in the code n ensures better performance but this randomness should be within a limit such that decoding feasibility is reliable. This is provided by interleaver in the turbo codes. In addition, these interleavers help reduce the number of low weight code words. They have high performance at low SNRs, however, they have BER error floors due to low minimum distance.

Encoding is done to improve the error correction capability. During encoding the redundancy bits are added to the codeword. This creates the rate of encoder output different than that of input information data rate. Here the data bits are encoded by the RSC encoder initially which is then rearranged using pseudo random interleaver followed by identical RSC encoder. Then the systematic output and the parity outputs of the two encoders are the data sequences which is passed through the channel. RSC encoders and the interleavers are considered as the important parameters for turbo coding [49, 51]. The low output weight due to interleaver and high output weight at next encoder output in overall gives larger free distance which signifies the lower BER.

3.8.1.1. Puncturing

Puncturing is carried out where certain parity bits are removed out of the given codeword sequences using some fixed rule or the puncturing matrix. These eliminated bits are replaced with zero instead of these bits before decoding. Advantageous factor for the puncturing is that it increases the data rate but does not increase the decoding complexity since the trellis of original code can be used [53]. The redundant bits used in the code word decreases the bandwidth efficiency. Though the puncturing process decreases the performance of system comparatively as random interleaver causes random protection of the parity bits but it increases the bandwidth efficiency of the system. Thus considered as a tradeoff between the rate and the performance. Puncturing pattern also decides the performance quality. When punctured, it causes less information bits to be transmitted which ultimately causes degradation in the code performance.

Rate compatible turbo coding is made possible with the puncturing process. The puncturing matrix used to change the code rate, represented by P of period p can be expressed as

$$P = \begin{bmatrix} g_{11} & \cdots & g_{1p} \\ \cdots & g_k & \cdots \\ g_{N1} & \cdots & g_{Np} \end{bmatrix}$$

where N denotes the output branches in which every row corresponds to one output branch. The term $g_{ik} \in (0, 1)$ in which 0 indicates the punctured bit. Increment in p increases the degree of freedom of controlling the code rate [54].

Different code rates are required depending on the situation where the coding is used. In the satellite communication, low code rates are preferred as the link reliability is very important in such scenarios whereas in other wireless communications, where bandwidth efficiency is of prime concern, high rate codes are desired. Code rate is increased by the periodic elimination of specific code bits. Puncturing pattern if arranged unsuitably can degrade the system performance due to uneven protection of information bits.

3.8.2. Decoder

Decoder basically produces an estimate of the transmitted bits in a way that probability of an individual bit is maximized. Turbo decoding uses an iterative approach to reduce the number of states. To make this feasible, it makes use of the soft decision approach instead of the hard decision. Hard decision is a way of choosing a sequence of 0 or 1 output bits based on the input symbols. On the other hand, soft decision refers the way in which the decision is produced as a value in $[0, 1]$ that corresponds to the likelihood (or log likelihood). It uses log likelihood ratio (LLR) as an input to decoder. The soft input soft output (SISO) processing used in the decoder which includes trelis diagram, shows the possible encoder sequences. LLR output from the first SISO is passed to second and vice versa to estimate the LLR outputs [55]. The MAP algorithm, also known as BCJR, APP, or backward-forward algorithm gives the computation of LLR relative to data d_i.

The traditional decoder produces hard decision of the received data symbols as 0 or 1 to the error control decoder. They are prone to error as different bits are determined with different level of certainty that makes decoder difficult to make the decision. The turbo codes rather uses SISO decoder which receives the soft decision (real value of the signal) and makes a decoder output for each data assuming the probability estimation for the transmitted data bit equal to 1 [56]. It consists of two decoders for both encoder output which gives estimates of the same set of data bits in different order. During decoding, if the intermediate values are soft values, the information exchange procedures provides coding gain and it passes soft decisions from the output of one decoder to the input of the other decoder. This process is done iteratively for reliable decisions which enhance the system performance. Turbo codes require an estimation of SNR to compute the LLR.

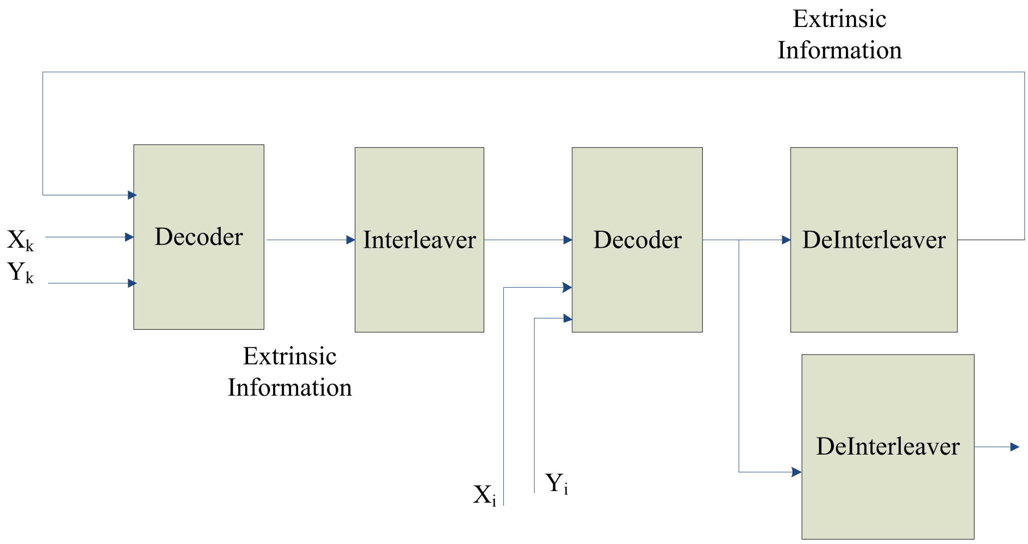

Figure 3.9: General block showing Turbo decoding [57].

As seen in the Figure 3.9, it contains two identical decoders connected through the feedback loop. These are the SISO decoders implementing the BCJR algorithm. The soft sequences for the data and parity bits are passed into these decoders. This yields the soft output sequence in the form of LLR. The measure of probability is defined as

$$\Lambda(d_i) = \ln \frac{P_r\{d_i = 1|R_1^k\}}{P_r\{d_i = 0|R_1^k\}}, \tag{3.26}$$

where R_1^k is the received noisy sequence, R_1^k = $\{R_1,...R_k\}$ with R_i =(x_i,y_i), d_i is the message bit associated with a transition in the trellis with 1 or 0. For value of d_i towards 1 or 0, output Λ_i is positive or negative. For equiprobable event, output is 0.

The interleaver used between the two decoders help to spread the residual error that arises due to the effect of first decoder. Due to this, the extrinsic information from second decoder is less correlated. Now, feeding this extrinsic information back to first decoder, the overall performance can then be increased. Repeating the process iteratively, the final output of LLR can be improved. This makes the decoder output more accurate and provide high gain.

MAP and the Soft Output Viterbi Algorithm (SOVA) algorithms are the two commonly used algorithms in turbo decoding procedures. They show similar performance at high E_b/N_0. However at low E_b/N_0, MAP algorithm outperforms the latter. MAP algorithm makes use of the search of most probable received bit using the conditional probability of the transition from the previous bit. This change in the state of the trellis brings the LLR probability as a suitable probability measure of MAP. MAP algorithms are preferred over the SOVA algorithms as they have better performance as compared to SOVA even at comparatively low E_b/N_0 [56]. Here E_b denotes the energy per information bit and N_0 is the noise power density.

Encoded outputs can be decoded iteratively at the decoder for better result. Iterative decoder differs from the other binary decoder in the way of implementation of first decoding step. These decoders first processes its encoders noisy output followed by next encoders noisy output. The outputs are then analyzed to get the final output. The decoder output contains three additive parts [58]. For each information bit k, it has the systematic component corresponding to received systematic value for given bit, the priori component which relates to the information from other decoder to that particular bit k and finally the extrinsic component which refers to the result from all other inputs. Usually the extrinsic part is passed through the next decoding to restrict the information to be used only once in the receiver [56, 58]. This makes turbo codes provide an astonishing performance of BER at relatively low E_b/N_0.

4. FTN SIGNALING AND SYSTEM MODEL

This chapter deals with the explanation of the transceiver structure that makes the benefits of FTN practically realizable. Transmission of the signals is carried out at higher data rate by sending more pulses at the given time period than the usual conventional method without deteriorating the system performance. The unavoidable inter symbol interference that occurs at the receiver is the issue to be addressed properly to receive the signals as close as possible to the transmitted signals. Complex receiver designing is required at the receiving end to overcome this issue. The thesis work is focussed to minimize the complexity of the receiver and still obtain the acceptable error performance of the system. The high data rate due to FTN comes as a trade off between throughput and error complexity. Minimizing the bandwidth occupancy by the transmitting signal and reducing the transmission time is the objective of the research work. In this thesis work, performance of the system at different FTN rates (time period) is analyzed and finally the FTN performance under the implementation of turbo coding is scrutinized.

4.1. System Model

The system model for the FTN transmission system discusses about the linear modulated transmission model and processing descriptions of faster than Nyquist signaling. The baseband representation of the signal

$$s(t) = \sum_{n=0}^{\infty} a_n h(t - nT) \tag{4.1}$$

can be represented in the FTN form as,

$$s(t) = \sum_{n=0}^{\infty} a_n h(t - n\alpha T); \alpha \leq 1. \tag{4.2}$$

The symbol time T is reduced to αT, where $\alpha T \leq T$. In equation (4.2), a_n refers the real and equiprobable independent and identically distributed (i.i.d) data and $h(t)$ is the T-orthogonal baseband pulse with real unit energy.

Power spectral density of the i.i.d symbols for above equation (4.2) can be written as

$$\phi_{sa}(f) = \frac{\sigma^2}{\alpha T} |H(f)|^2, \tag{4.3}$$

where $\sigma^2 = \mathbb{E}[|a_n|^2]$.

The average power thus can be defined by the relation

$$P = \frac{\sigma^2}{\alpha T}. \tag{4.4}$$

Here the signaling rate is defined by $1/\alpha T$ Hz and the FTN rate is given by $1/\alpha$, $0 < \alpha \leq 1$. If $\alpha = 1$, then the system is orthogonal which describes the ISI free Nyquist signaling. But in the thesis, $\alpha < 1$ is assumed which refers to the FTN signaling. The signaling time in this case is thus defined by $\alpha T < T$. The general block diagram describing the system model is presented in Figure 4.1.

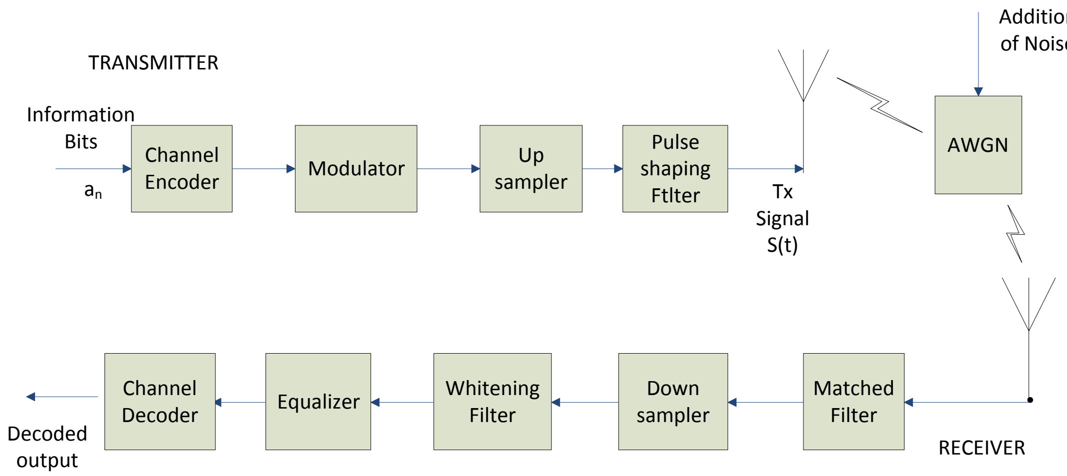

Figure 4.1: General block diagram for system model.

4.1.1. Transmitter

This section concentrates on the transmitter side of the system model and the signal processing of the transmitted waveform. The information signal is required to be modified in a way that it meets the requirements of signal transmission. Various signal processing techniques are implemented to introduce FTN to the transmitted signals. The transmitter block consists of different parts which are discussed below.

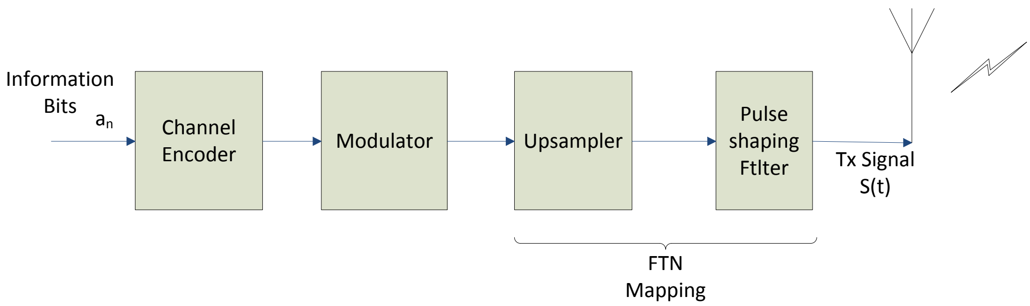

Figure 4.2: General block diagram for the FTN Transmitter.

Figure 4.2 shows the basic block structure for the FTN transmitter system. At first, the uncoded signal is passed through channel encoder. The channel encoded signal as a result of the encoder is modulated to generate the binary phase-shift keying (BPSK) signals as of the interest. Let b denote the modulated signal where M-ary modulation is done and finally $s(t)$ denotes the transmitted signal after the FTN mapping. System performance for both the coded and the uncoded input signals are analyzed.

Pulse amplitude modulation enables the information to be embedded in the amplitude of the carrier pulse. The modulation can be used for both base band and pass band signals. Transmitted data is represented as a block of data. For baseband signal, it can be represented as

$$s(t) = \sum_{n=1}^{N} a_n g(t - nT), \tag{4.5}$$

where $a_n = \pm 1, \pm 2...$ denotes the amplitude carrying the signal information.

For FTN transmission systems, the time period for the signal transmission is reduced by certain factor. Equation (4.5) can therefore be deduced into

$$s(t) = \sum_{n=1}^{N} a_n g(t - n\alpha T). \tag{4.6}$$

The signal for transmission thus generated, is sampled by the proper sampling procedures. Sampled signals are mapped with an upsampler of factor N and a pulse shaping filter $h(t)$ which is symmetric. It has a unit energy, i.e.,

$$\sum_{-\infty}^{\infty} |h[n]|^2 = 1. \tag{4.7}$$

The effect of upsampling and pulse shaping filter is combinedly introduced as FTN mapping.

For FTN transmission, $\alpha T < T$. In the equation (4.6), the term αT is the new time period instead of T which indicates that the time period is reduced. This implies that the pulses are no longer orthogonal. As a consequence, it produces an undesired ISI which is to be minimized.

For creating a FTN scenario, it is upsampled by a factor K where $N < K$. This provides the FTN rate which is calculated by the ratio $\frac{K}{N}$ [1]. The term α which modifies the FTN time period is given by $\alpha = \frac{N}{K} < 1$. If these upsampling points are not estimated properly, they give rise to ISI. It indicates the distortion faced when the transmitted symbols overlap partially or totally thereby causing the degradation of the system by reducing the detection performance of receiver [2]. FTN symbols as it contains non-orthogonal signals are subjected to such ISI.

Upsampling involves the addition of $(N - 1)$ zero samples between every sample of the input. This scales the time axis by factor N. In frequency domain analysis, this means the scaling of frequency axis by factor $1/N$.

FTN mapping involves upsampling of a modulated signal and its response after passing through the pulse shaping filter. The upsampled signal and the pulse filter generated response can be defined as,

$$\begin{aligned} s(t) &= \sum_{k=0}^{\infty} b_k h(t - k\alpha T), \\ v[n] &= \begin{cases} b(n/N) & n = 0, N, 2N \\ 0 & otherwise\ . \end{cases} \end{aligned} \tag{4.8}$$

Here, $v[n]$ is an upsampled signal response and $s(t)$ is the signal response at an output of the pulse shaping filter used.

Pulse shaping in the thesis work is done using the raised cosine pulse as a pulse shaping filter. Pulse shaping filters are selected considering the requirement that they satisfy the Nyquist ISI criterion. The selected, unit-energy raised-cosine T-orthogonal pulse ensures the pulse shape $h(t)$ provide an ISI free transmission. Raised cosine pulse is preferred over the Sinc pulse since the Sinc pulses decay faster. The Sinc pulses have faster decaying nature in frequency domain and infinite impulse response in time domain. Raise cosine pulses, on the other hand, has necessary pulse bandwidth and also satisfies the Nyquist condition. Raised cosine is implemented as a combined effect of root raised cosine used as a pulse shaping filter at the transmitter and as a matched filter at the receiver.

In order to have the signal $y[n]$ fulfill the Nyquist condition, for $y[n] = x[Kn]$, $y[n]$ should satisfy

$$y[n] = \begin{cases} 1/K & n = 0 \\ 0 & n \neq 0. \end{cases} \tag{4.9}$$

This implies $Y(e^{j\omega}) = 1/K$. Using discrete time Fourier transformation (DTFT),

$$\begin{aligned} Y(e^{j\omega}) &= \frac{1}{K}\sum_{k=0}^{K-1} X(e^{j\frac{\omega}{k}-\frac{2\pi}{K}k}) \\ or,\ &\sum_{k=0}^{K-1} X(e^{(j\omega/K)-(2\pi/K)k}) = 1. \end{aligned} \tag{4.10}$$

Fulfilment of this criteria means that signals are orthogonal, i.e., for a given impulse response, sampling instants having only one non zero sample. Now for the Nyquist pulse any shift orthogonal pulses can be used by convoluting itself with time or multiplication in frequency domain. Root raised cosine pulses are such pulses used in the thesis work. RRC pulse is defined by

$$h(t) = \frac{4\beta}{\pi\sqrt{T_0}} \frac{\cos\frac{(1+\beta)\pi t}{T_0} + \frac{T_0}{4\beta t}\sin\frac{(1-\beta)\pi t}{T_0}}{1-(4\beta t/T_0)^2}\ . \tag{4.11}$$

RRC pulse is the square root of the Fourier transformation of the RC pulse. For FTN transmission, the time period is modified as $T_0 = \alpha T$. The factor $(1 + \beta)$ in equation (4.11) stipulates the fact that it is not as efficient as Sinc pulse regarding the spectral efficiency (resembles Sinc pulse for $\beta = 0$). These are sampled and processed to the matched filter at the receiver relating it as a Nyquist filter. The bound for the realistic raised cosine filter is given by $T_0 = (1 + \beta)/(2B)$ [5]. Roll-off factor is defined between 0 and 1, i.e., $\beta \in (0, 1)$.

The RC pulse transmission at Nyquist rate and FTN rate is expressed in the Figure 4.3. Sending the raised cosine pulse at two different approaches, i.e., at the Nyquist rate $1/T$ and at FTN rate $1/\alpha T$, the study of the pulse shows different nature. Following the perfect Nyquist condition, the pulse amplitude is summed up to 1 as explained in equation (4.10). For the case of rectangular pulse limited from $-1/2T$ to $1/2T$, using the anti-aliasing low pass filter at the receiver, the original signal can be reconstructed perfectly. This ensures that the full information is retained. However, for the case where FTN is applied in time domain, the frequency domain are shifted apart. For such condition, in order to reconstruct the original signal, a low pass filter having bandwidth B larger than $1/T$ is required.

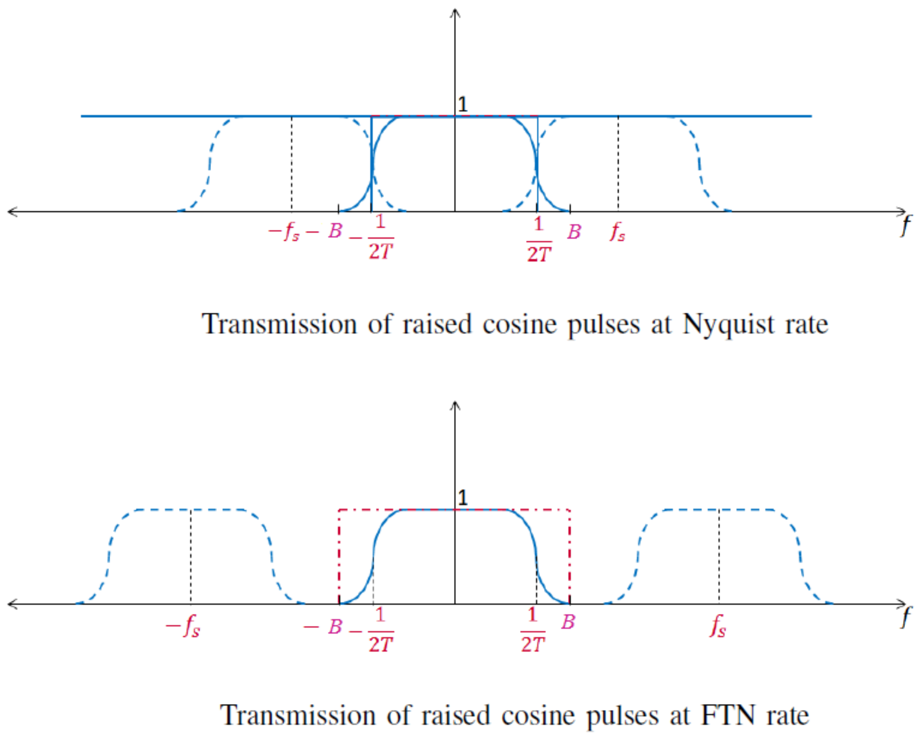

Figure 4.3: Raised cosine pulse at different condition [1].

The sampled form of autocorrelation function can be written as,

$$h_{xx}(l) = \sum_{n=-\infty}^{\infty} x[n]x[n-l]. \tag{4.12}$$

In the equation (4.12), if $h[l] = \delta[n]$, then the pulse $h[n]$ becomes orthogonal. However, if $h[n] \neq \delta[n]$, it introduces ISI. These ISI are the undesired terms which make the receiver processing a complex task. From the transmitter side, it is tried for the pulse $h[n]$ which gives $h[n] = \delta[n]$, provide the narrow PSD. The narrowest PSD with T-orthogonal pulse is contained by the Sinc pulse.

However, root raised cosine pulses are preferred due to the practical limitations of the Sinc pulses. The frequency domain representation for the RRC pulses used as pulse shaping filter is given by

$$|H(f)|^2 = \begin{cases} T & , \quad |f| \leq (1-\beta)/2T \\ T\cos^2\left(\frac{\pi T}{2\beta}\left(|f| - \frac{1-\beta}{2T}\right)\right) & , \quad (1-\beta)/2T < |f| \leq (1+\beta)/2T \\ 0 & , \quad |f| > (1+\beta)/2T. \end{cases} \tag{4.13}$$

Fourier transform of these RRC pulses is antisymmetric at point $f = 1/2T$. The PSD as defined in equation (4.3) is maintained constant to assure the fair comparison of FTN system. During FTN transmission, the time period is considered as αT. For the practical implementation, the trunks of the RRC pulses are truncated to make them physically realizable.

For the data transmitted following the orthogonality principle, ISI free response is received as each data will be sent independently. However, while implementing FTN, the orthogonality principle can no longer be preserved.

4.1.1.1. Normalization of energy

In FTN, the data pulses are transmitted in a compact form, i.e., more symbols are sent for the given time period. Comparatively, more samples/symbol are sent. This situation may require to increase the transmitted symbol power. However, to make sure of the fair comparison of FTN signaling, instead of increasing the power, pulse energy is normalized making the power constant.

4.1.2. Receiver Design for FTN with MMSE equalizer

Now considering the AWGN channel, for the estimation of the information sequence a_n, the following expression describes the received signal $y(t)$ such that

$$y(t) = s_n(t) + n(t). \tag{4.14}$$

Output sequence $r(t)$ thus can be expressed as,

$$r(t) = \int_{-\infty}^{\infty} y(t)h^*(t - n\alpha T)dt. \tag{4.15}$$

The above equation (4.15) can be represented in a matrix notation as

$$r^N = G^N a^N + \eta^N. \tag{4.16}$$

Here G^N represents $N \times N$ toeplitz matrix defined by $\{g[0], g[1], ...g[N-1]\}$, a^N represents $\{a[0], a[1], ...a[N-1]\}^T$ and η represents the colored gaussian noise.

Here,

$$g[k] = \int_{-\infty}^{\infty} |H(f)|^2 e^{j2\pi k\alpha T f} df. \tag{4.17}$$

The term $e^{j2\pi k\alpha T f}$ is periodic and the term $1/\alpha T$ is the multiple of period. The term $g[k]$ can then be deduced as,

$$g[k] = \sum_{k=-\infty}^{\infty} \int_{-1/2\alpha T}^{1/2\alpha T} |H(f + k/\alpha T)|^2 e^{j2\pi k\alpha T f} df. \tag{4.18}$$

Now rearranging the summation and integral operation, we get,

$$\begin{aligned} g[k] &= \int_{-1/2\alpha T}^{1/2\alpha T} \sum_{k=-\infty}^{\infty} |H(f + k/\alpha T)|^2 e^{j2\pi k\alpha T f} df \\ &= \int_{-1/2\alpha T}^{1/2\alpha T} |H_{fold}(f)|^2 e^{j2\pi k\alpha T f} df \ . \end{aligned} \tag{4.19}$$

The folded spectrum $|H_{fold}(f)|^2$ is considered zero outside the interval $-1/2\alpha T \leq f \leq 1/2\alpha T$, i.e.,

$$|H_{fold}(f)|^2 = \sum_{k=-\infty}^{\infty} |H(f + k/\alpha T)|^2, \quad \frac{-1}{2\alpha T} \leq f \leq \frac{-1}{2\alpha T} \ . \tag{4.20}$$

For $g[n] \neq \delta[n]$, $[g_{-}2, ...0, ...g_2]$ represents the ISI.

The shape of $H(f)$ is related with the y^N formed from generator matrix G^N. This infers that the transfer function for $H(f)$ produces equivalent g which stipulates that $H(f)$ and H_{fold} are interchangable [59]. The function $H(f)$ shows equivalent statistical detection.

The average power of the transmission is given by relation

$$P = \frac{\sigma^2}{\alpha T}. \tag{4.21}$$

In this scenario, the faster data rate due to FTN is equivalent to the procedure of transmitting the comparatively wider pulse in time. For the pulse widened by the factor $1/\alpha$ the pulse becomes T' orthogonal for $T' = T/\alpha$. The pulse is represented by,

$$h_w(t) = \sqrt{\alpha}h(\alpha t). \tag{4.22}$$

The signal $s(t)$ is transmitted in an AWGN channel. The received signal at the receiving end is thus defined by

$$y(t) = s(t) + \omega(t), \tag{4.23}$$

where $\omega(t)$ is the white noise with mean zero and noise spectral power density of $N_0/2$.

More specifically, the receiver designing is discussed with the help of system model for the receiver section as described in the Figure 4.4.

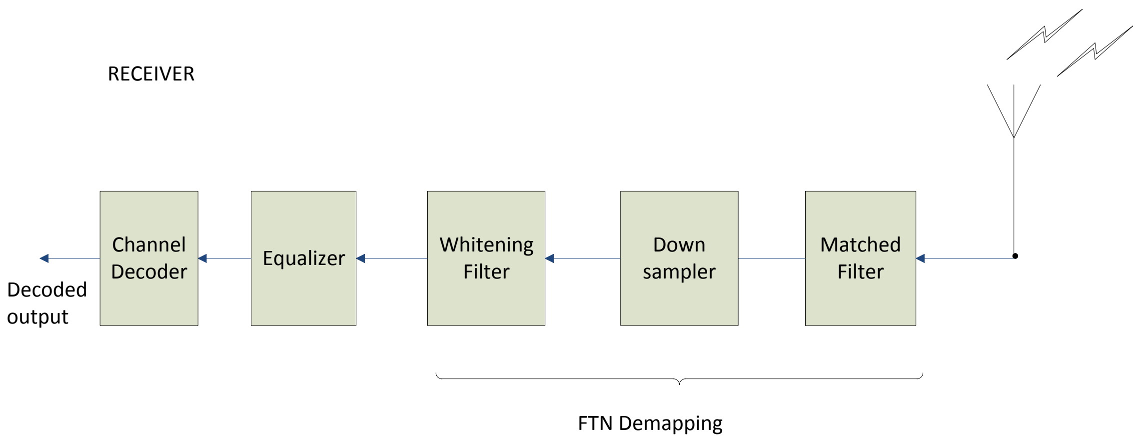

Figure 4.4: General block diagram for FTN receiver model.

It considers the building blocks for the receiver end of the FTN transmission systems. The received signal $y(t)$ first faces the FTN demapping. This demapper provides symbol rate for the received signal. The received signal $y(t)$ undergoes the demapping processing as shown in the Figure 4.4. The result out of this demapping block is represented by $r(t)$ which can be expressed as,

$$\begin{aligned} r(t) =& y(t) * h^*(-t) \\ =& (s(t) + \omega(t)) * h^*(-t) \\ =& (\sum_{k=0}^{\infty} b[k]h(t - k\alpha T)) * h^*(-t) + \omega(t). \end{aligned} \tag{4.24}$$

The signal is sampled for every αT. Using the same pulse shapes as that of the pulse shaping filter of the transmitter side, matched filtering $h^*(-t)$ is carried out for the received signal $y(t)$. The resulting signal $r(t)$ is then finally downsampled by the factor N. Whitening filter is used to whiten the colored noise. In the equation (4.24), $\omega(t)$ is the colored noise. The FTN process creates the ISI which is dealt with equalizer to mitigate the effects of such unwanted ISI. The soft output bits are generated out of the equalizer which is passed to the channel decoder.

FTN demapper consists of matched filter, desampler and the whitening filter. The sampled data is generated from the received continuous signal $r(t)$. This is done in the matched filtering process. In reference to the upsampler used at the transmitter, receiver involves downsampler. Downsampling involves the removal of zero samples (i.e., scaling of time axis) which indicates the scaling of frequency axis by factor N. Using shift orthogonal pulses, the received structure can be represented as

$$\begin{aligned} r_n =& (y(t), h_T(t-nT)) \\ =& (s(t), h_T(t-nT) + (\omega(t), h_T(t-nT) \\ =& \underbrace{\sum_m a_m (h_T(t-mT), h_T(t-nT)}_{a_n} + \eta_\eta . \end{aligned} \tag{4.25}$$

Here a_n represents the information signal amplitude. The matched filter is matched with the pulse $h(t)$ and this is sampled at the rate $1/\alpha T$. The basic representation of signal flow in matched filter is shown in Figure 4.5. The term η_η represents random independent gaussian noise with variance $N_0/2$. It can be simply represented by, $r = a + \eta$, where r is the received signal and η is the i.i.d. gaussian noise vector. The case is assumed to be for the ideal situation having unit energy pulses. However, for the situation where varying input power is desired, it can be achieved by using square root of power, i.e., $\sqrt{P}$ as $r = a + \sigma\eta$, where $\sigma = \sqrt{N_0/2P}$. The term σ^2 denotes the variance which is defined by the inverse of linear SNR, i.e.,

$$\begin{aligned} \sigma =& \sqrt{N_0/2P} \\ =& 10^{-SRN/20}(dB). \end{aligned} \tag{4.26}$$

The sampled noise having smaller value of standard deviation implies that the samples are near to the actual values thereby making the estimation more accurate.

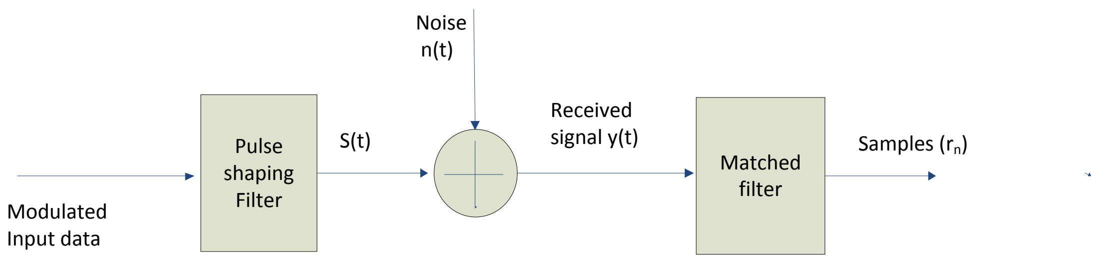

Figure 4.5: Block diagram showing signal processing with matched filter.

After the matched filtering, there comes a whitening filter. This receiver filter is also matched to $h(t)$ and sampled at each αT. For the further discussion, for equation,

$$x = a * g + \eta,$$

$$g_k = \int h(t)h(t + k\alpha T)dt, \tag{4.27}$$

where g is the sampled autocorrelation function of $h(t)$ and η is the colored gaussian noise. The z transform for above equation (4.27) can be written as

$$x(Z) = A(Z)G(Z) + N(Z). \tag{4.28}$$

Now using the spectral factorization of $G(z)$ into $v(z)v^*(1/z^*)$, the whitening filter is constructed. This decorrelates the colored noise η. So the whitening filter $1/v^*(1/z^*)$ is used. This gives the modified relation as

$$\tilde{y} = a * v + \omega, \tag{4.29}$$

where ω is the white gaussian noise with variance $N_0/2$.

4.1.2.1. Mean square error estimation

Initially, the probability of error is minimized. Estimate of x is determined to ensure low error probability for the data y with sent data vector a, i.e., x is calculated for the received signal $r(t)$ such that it minimizes

$$min_x P(x \neq a|r(t)).$$

Here,

$$P(x \neq a|r(t)) = 1 - P(x = a|r(t)).$$

This is equivalent to,

$$max_x P(x = a|r(t)).$$

Using the Baye's rule,

$$\begin{aligned} P(a|y) &= \frac{P(y|a)P(a)}{P(y)} \\ &= argmax_a \frac{P(y|a)P(a)}{P(y)} \\ &= argmax_a P(y|a). \end{aligned} \tag{4.30}$$

Here $P(a)$ and $P(y)$ are independent of a. The likelihood is defined by $P(y|a)$. Thus maximum likelihood estimation (MLE) defines the estimation giving minimum error probability. So for the pulses with information sequence a_n of N independent pulses, there exists vector a that maximizes expression for each component near to y. This can be mathematically written as,

$$x_n = min_{a_n}(y_n - a_n)^2.$$

4.1.2.2. Minimun mean square error equalizaion

In case of FTN signaling, both the non white noise and the ISI are to be taken into account for the receiver design. The whitening filters are therefore followed by the equalizers. FTN signaling makes use of the compact form of signals, i.e., they contain comparatively more symbols for the given time period T than the conventional orthogonal systems. This yields the ISI. So the linear MMSE equalizers are implemented to get rid of this interference.

For the information symbol a_n, where n is the symbol index, modulated with l coded information bits, the transmission is carried out through the T orthogonal pulse shaping filter $h(t)$. Each symbol is convolved with the shaping filter $h(t)$ and the signal is transmitted at the symbol interval $T_0 \leq T$. Pulse shaping is done using the RRC filters. The average energy of the symbol is thus given by the relation, $E_s = E\{|a_n|^2\}$. The individual symbol is transmitted at the interval of αT, i.e., signaling rate equals to $1/\alpha T$. In the relation, α is maintained less than 1 for FTN transmissions which indicates the ratio of the symbols compact or the symbol packing ratio. For the case of orthogonality, $\alpha = 1$. This indicates that ISI does not exists. As α decreases, the rate of transmission increases but at the cost of increased error, which needs to be equalized. The MMSE equalizers treat the data symbols as random variables having mean and variance calculated from the a priori information.

For the information sequence transmitted at FTN transmission scheme, the received signal under the assumption of AWGN noise is given by

$$y(t) = \sqrt{E_s} \sum_n s_n g(t - nT_0) + \eta(t), \tag{4.31}$$

where

$$g(t) = \int h(\alpha) h^*(\alpha - t) d\alpha \quad \text{and}$$
$$n(t) = \int n(\alpha) h^*(\alpha - t) d\alpha \; .$$

Here s_n is the information symbol, $h(t)$ is the impulse response of shaping filter, n is the symbol index, $n(t)$ is the guassian distributed complex random variable $CN(0, N_0)$ with zero mean and variance N_0, E_s the average power for the transmitted symbols and $T_0 = \alpha T$, where α is the symbol packing ratio. Now under the assumption of perfect synchronization between the transmitter and receiver, the received signal for k^{th} sampled signal is given by

$$\begin{aligned} y_k &= y(kT_0) \\ &= \sqrt{E_s} \sum_n s_n g(kT_0 - nT_0) + \eta(kT_0) \\ &= \sqrt{E_s} s_k g(0) + \sqrt{E_s} \sum_{n \neq k} g(kT_0 - nT_0) + \eta(kT_0) \end{aligned} \tag{4.32}$$

In the equation(4.32), the first term represents the symbol of interest and the second term refers to the ISI. If symbol packing ratio $\alpha = 1$, then this second term would disappear as it would be perfect Nyquist condition. Now, retaining the high normalized rate of FTN, we use frequency domain equalization technique to overcome this unavoidable ISI. The efficient fast Fourier transform (FFT) used in FDE also aids in handling the channel impulse response spread over large range of symbols. Since the uncoded FDE for the FTNs receiver does not meet the optimal performance, some coding techniques can be beneficial.

It considers the implementation of finite-tap equalizers to compensate linear ISI in the presence of additive white Gaussian noise. For the received signal r_k and input sequence estimate $\hat{a_k}$,

$$MSE = E[|r_k - \hat{a_k}|^2]. \tag{4.33}$$

These equalizers de-convolves the linearly distorted channel along with the transversal filter in a way that it generates an inverse of the channel. The equalizer output is quantized to reconstruct the original transmitted symbols. The error estimation is given by

$$e(k) = r(k) - a(\hat{k}).$$

Now the minimization of $E|e[k]|^2$ is required.

Finally the MMSE equation for linear filter in frequency domain is given by,

$$C(z) = \frac{H^*(z)}{H(z)H^*(z) + \sigma^2}, \tag{4.34}$$

where $H(z)$ represents the pulse frequency response, * represents conjugate operation and σ^2 is the noise variance.

Frequency domain equalization offers an advantage over its corresponding time domain in the sense that fast convolution can be carried out in frequency domain reducing the processing operations. Unlike the time domain where each tap weight is related to the entire set of channel impulse response for all delays, the frequency domain response of the equalizer is related with the channel response corresponding to that particular instant of frequency and its additional alias frequency. In addition to this, the frequency domain algorithms are faster and more stable [60].

4.1.3. Receiver design for FTN transmission with turbo coding

The high data rate due to FTN is possible at the cost of increased ISI. This situation stipulates the need of an efficient FTN equalizer at the receiving end. For the uncoded system, this increment in the rate due to FTN is directly related to lowering the value of FTN time period $\alpha = T_0/T$. But at the same time, this creates the degradation of the BER performance of the system. For the BPSK modulation of the signals with root raised cosine pulse as a pulse shaping filter, the FTN performance is scrutinized with MMSE equalization as explained in section 4.1.2.

In order to compensate this loss due to ISI, some channel coding techniques like turbo codes, LDPC codes can be implemented. In this part of work, turbo coding is utilized and the performance is evaluated. Turbo coding makes use of an iterative decoding of these error correcting codewords. The transmitter and receiver model is assumed considering an AWGN channel with the code rate r. The ISI effect which is produced due to FTN transmission is mapped to a trellis structure and finally analyzed using the iterative turbo decoder following BCJR algorithm.

These high-performance FEC codes have the performance much better than the corresponding convolution code. The turbo codes makes use of RSC encoder and iterative BCJR decoder. RSC turbo encoder contains the encoder and an interleaver.

At the transmitter side, the source coded data bits are passed through an encoder which produces encoded data bits. Turbo encoder used for the thesis work is with rate $1/3$. The pseudo random interleaver is used for generating the interleaved data bits.

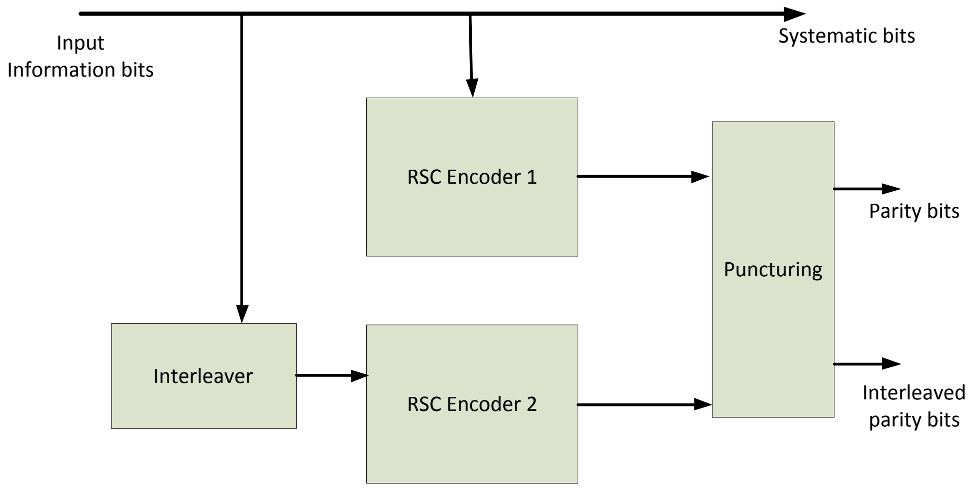

Figure 4.6: Basic block of Turbo encoder with rate $1/3$.

As seen in the Figure 4.6, the encoder consisting one input information of sequence of length N and three output sequences is used. It has the coding rate $1/3$. Input data is encoded to produce three different outputs as systematic, first parity and second parity sequences. In the thesis work, code rate of the turbo code is varied in order to analyze the performance of the system at different conditions. This is done by the process of puncturing. Using the puncturing pattern to modify the encoded data, the code rate is increased. To make the fair comparison during the result analysis, FTN rate and the code rate is manipulated to make the overall rate equivalent at different situations.

The generator polynomial function for the encoder is defined by

$$G[D] = \begin{bmatrix} 1 & \frac{1+D+D^2}{1+D^2} \end{bmatrix}$$

The encoder structure contains three different forms of encoder output. The first encoder generates the parity bit from the input information bits. It is denoted by $\overline{P_0}$. Likewise, next encoder generates the parity bit $\overline{P_1}$. The interleaver used changes the pattern of the input and generates the interleaved version of the input data $\overline{X_\pi}$ from $\overline{X}$.

Mathematically, it is represented as,

$$\begin{aligned} \overline{X} &= X^0 X^1 ... X^{n-1} \\ \overline{X}_\pi &= X_\pi^0 X_\pi^1 ... X_\pi^{n-1}. \end{aligned} \tag{4.35}$$

It comprises of the information bits $X(D)$ and the parity bits

$$X(D)\frac{1+D+D^2}{1+D^2} = P_0^0 P_0^1 ... P_0^{N-1} \quad and$$
$$X_\pi(D)\frac{1+D+D^2}{1+D^2} = P_1^0 P_1^1 ... P_1^{N-1}.$$

Now considering $C_0(D) = X(D)$, $C_1(D) = X(D)\frac{1+D+D^2}{1+D^2}$, and $F(D) = \frac{X(D)}{1+D^2}$, we get the relation,

$$\begin{aligned} C_0^j &= X^j \\ C_1^j &= X^j + F^{j-1}. \end{aligned} \tag{4.36}$$

In the above relation (4.36), $F^j = F^{(j-2)} + X^j$. The encoded code word from the encoder can therefore be given by,

$$\overline{C} = X^0 P_0^0 P_1^0, X^1 P_0^1 P_1^1, ... X^{N-1} P_0^{N-1} P_1^{N-1}. \tag{4.37}$$

System model including the turbo code shows that the encoded data bits are passed through the modulator. The signals are BPSK modulated before they are finally passed into the pulse shaping filter. The modulation in this case can be expressed as

$$\begin{aligned} u_0^j &= 2X^j - 1 \\ u_1^j &= 2P_0^j - 1 \\ u_1^j &= 2P_1^j - 1, \end{aligned} \tag{4.38}$$

where $j = 0, 1, 2...N-1$. Puncturing matrix is used as shown in the Figure 4.6 to modify the encoded bits such that the code rate is increased. The number of bits transmitted is reduced as compared to non punctured bits without reducing information bits. This causes the rate to be increased. Puncturing matrix (P) used for changing the code rate is given by,

$$\mathbf{P} = \begin{bmatrix} 1 & 1 & 1 \\ 1 & 1 & 1 \\ 1 & 1 & 1 \\ 1 & 1 & 1 \end{bmatrix}_{code\ rate\ 1/3} \qquad P_{punctured} = \begin{bmatrix} 1 & 1 & 1 \\ 1 & \times & 1 \\ 1 & 1 & 1 \\ 1 & \times & \times \end{bmatrix}_{Punctured\ rate\ 4/9}$$

In the matrix, $\times$ denotes the punctured bit.

In the matrix P, the first column, second column and third column represents the information bits, parity bits from first encoder and the interleaved parity bits respectively. The rate is thus defined as $k/n = 4/12 = 1/3$, where k and n represents the information bits and the total (including information and parity) bits respectively. Now using the puncturing matrix $P_{punctured}$, some parity bits are removed from the matrix in the pattern as shown such that rate r changes to $4/9$. Turbo code with changed rate is created to make the fair comparison between the coded systems using FTN and coded Nyquist satisfied scenarios. In the first case ,the turbo code with rate $1/3$ is modified with puncturing matrix to generate the code rate $4/9$ and FTN rate 1 is used making the overall rate equal to $4/9$. In the second case, turbo code with rate $1/3$ and the FTN rate $8/6$ is used making the same overall rate equal to $\frac{1}{3} \times \frac{8}{6} = 4/9$. This provides an environment for the fair comparison between the two approaches.

At the receiving end, decoding of the received code words is performed. Received signal in our case is the equalized output from the MMSE equalizer. It uses the BCJR algorithm. The BCJR decoder architecture contains two decoders for the corresponding two encoders. The inputs for the decoder is represented by $\overline{R_0}$ and $\overline{R_1}$ for the first decoder and $\pi\overline{R_0}$ and $\overline{R_2}$ for second decoder, respectively.

The log aposteriori probability ratio(LAPPR) is thus defined as

$$\begin{aligned} \Lambda^k &= log\frac{P(X^k = 1|\overline{R})}{P(X^k = 0|\overline{R})}, \\ \Lambda_1^k &= \Lambda^k - log\frac{P(X^k = 1)}{P(X^k = 0)} - \frac{2R_0^k}{\sigma^2}, \end{aligned} \tag{4.39}$$

where $\overline{R}$ is the input to decoder and $k = 0, 1, 2...N-1$.

For the first BCJR decoder, the input is represented by $R = \overline{R_0}\ \overline{R_1}$. We have the relation,

$$P(X^k = i|\overline{R}) = \frac{1}{P(R_0^{N-1})}\sum_{m=0}^{M-1}\sum_{m'=0}^{M-1}\alpha_k(m')\gamma_k^i(m', m)\beta_k(m). \tag{4.40}$$

In the equation (4.40), m and m' are stages (s_k) , M is the total number of stages and $i = 0$ or 1 (input). The terms $\alpha_k(m')$, $\beta_k(m)$ and $\gamma_k^i(m', m)$ represents forward state metric, backward state metric, and transition probability from state m' to m at stage k for input i, respectively, i.e.,

$$\alpha_k(m') = P(S_k = m'|\overline{R_0^{k-1}}) \ = \sum_{m''=0}^{M-1}\sum_{i=0}^{1}\gamma_{k-1}^i(m'', m)\alpha_{k-1}(m''), \tag{4.41}$$

$$\beta_k(m) = P(\overline{R_{K+1}^{N-1}}|S_{k+1} = m) \ = \sum_{m'=0}^{M-1}\sum_{i=0}^{1}\gamma_{k+1}^i(m', m)\beta_{k+1}(m'), \tag{4.42}$$

$$\begin{aligned} &\gamma_k^i(m', m) = \\ &\quad \underbrace{P(X^k = i)}_{\substack{\text{Apriori probability}\\ \text{at time k for input i}}}\ \underbrace{P(S_{k+1} = m|S_k = m', X^k = i)}_{\substack{\text{contribution from}\\ \text{trellis}}}\ \underbrace{P(\overline{R^k}|S_{k+1} = m', S_k = m, X^k = i)}_{\substack{\text{contribution from}\\ \text{likelihood}}}. \end{aligned} \tag{4.43}$$

The equations (4.41), (4.42) and (4.43) in addition with the apriori probabilities for inputs 0 and 1, is used to calculate the LAPPR for all stages and decoding of the codewords. At all stages for both the inputs, the output from the first decoder is passed to the second decoder. This helps to calculate the priory probability using LAPPR values. The process is continued iteratively until both the decoders have similar or the priory probability is 1 for one of the input. The values of α, β, and γ is used to determine the value of Λ^k for all the stages, i.e.,

$$\begin{aligned} P(X^k = 1) &= \frac{e^{\Lambda_1^k}}{1 + e^{\Lambda_1^k}}, \\ P(X^k = 0) &= \frac{1}{1 + e^{\Lambda_1^k}}. \end{aligned} \tag{4.44}$$

The BCJR algorithm and the interleaver arrangements for the BCJR output stands for the main role at the decoder. The algorithm computes the LAPPR for the convolutional code symbols which gives the aproiori probabilities of the symbol with respect to each other. The probabilities are produced in the form of series of iterations that ultimately converges for the LLR to represent the correct codeword [6].

In FTN, increase in the data rate is achieved at the cost of an unavoidable ISI which imposed the processing difficulties. However, with the use of these FEC turbo codes, receiver processing is justified with the benefits of FTN gain added with some coding gains.

5. MATLAB IMPLEMENTATION AND SIMULATION RESULTS

This chapter concentrates about the simulation setup environment for the performance analysis of the FTN transmission system. The results are presented for two different approaches. Firstly, the FTN transmission results of an uncoded system is kept forward. Then the comparative study for the system introducing the coded transmission is presented. The fair comparison of the coded system is ensured by providing the same rate of transmission for the coded system under usual Nyquist conditions and FTN transmission systems. As stated in [61], FDE provides lower complexity than its corresponding time domain equalization. Therefore, the receiver designing task is implemented utilizing the frequency domain characteristics.

5.1. FTN analysis under an uncoded system

The uncoded binary modulated signals are transmitted as an information bearing signals. These signals are designed in a way that they are transmitted at a rate faster than the rate prescribed by Nyquist criterion by introducing some oversampling factors. The upsampled signals thus created during FTN mapping defines the FTN scenario. These signals are introduced to FTN environment by using an upsampler of factor N and upsampled by the factor K, where $N < K$. The ratio $\frac{N}{K}$ defines the FTN rate. The signals are then introduced to pulse shaping filter. The Nyquist condition satisfying root raised cosine pulse is used to shape the modulated signal before transmission. The pulses are ensured that they really meet the Nyquist criteria. At the receiving end, the received signals are matched using the matched filter which is addressed with the corresponding down sampling procedures as reference to the up sampled signals. ISI free property of RC pulse comes after implementing the combined effect of RRC pulses as a pulse shaping filter at transmitter and as a matched filter at the receiver. The whitening filters are used to mitigate the effects of the colored noise. Finally, the MMSE equalizer is used to equalize the received signals. These equalized resulting signals are then compared with the original transmitted signals. The BER calculation of the signals is used to analyze the system performance.

5.1.1. Results

The MATLAB simulation plots are presented to analyze the results at different condition of FTN signaling. In the simulation results, alpha (α) denotes the FTN factor where symbol duration T is reduced to αT, $\alpha \leq 1$. For $\alpha = 1$, it represents the scenario satisfying Nyquist condition.

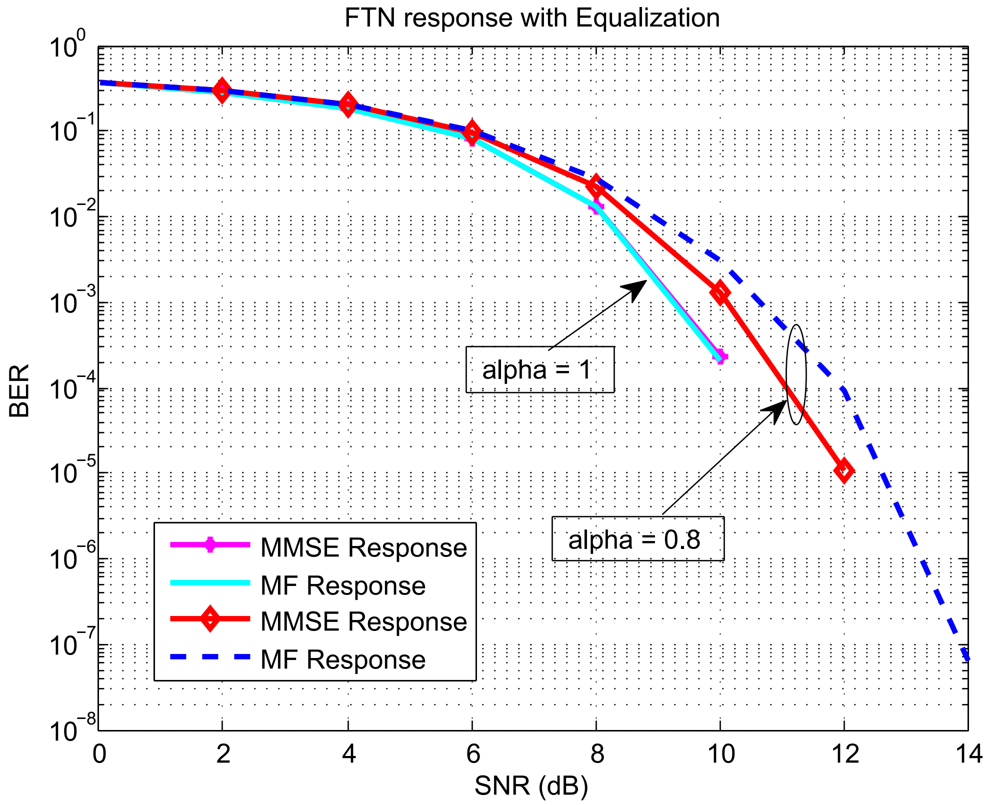

Figure 5.1: Comparison for Nyquist and FTN response with MMSE equalizer.

Figure 5.1 contains the plots for normal Nyquist condition satisfying transmission and the introduction of FTN signaling with FTN factor $(\alpha) = 0.87$. For $\alpha = 1$, the Nyquist signaling shows that MMSE equalizer response and matched filter (MF) response are equivalent. This indicates that equalizer has no significant role for such transmissions as there occurs no ISI since the signals are perfectly orthogonal. The signal degradation for the case with $\alpha = 0.87$ is due to the generation of ISI which is created as a consequence of FTN signaling as FTN makes the signal non orthogonal. In this case, equalizer has the dominant effect. MMSE equalizer mitigates an effect of ISI, therefore shows an improvement over the MF output.

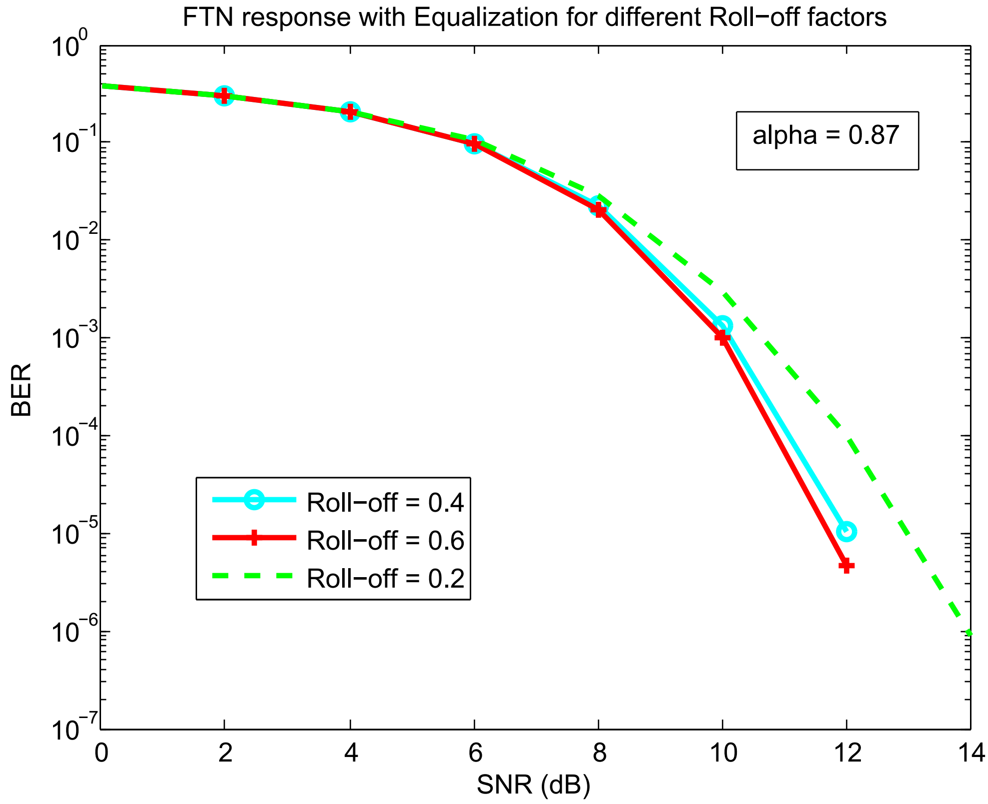

Figure 5.2: MMSE response of FTN signals for different roll off values.

The comparative analysis for the equalizer response as affected by the roll-off factors is shown in Figure 5.2. Higher roll-off (β) value provides good signal response but it comes at the cost of large bandwidth occupancy. If an acceptable error performance is achieved at the lower roll-off then it provides the comparatively better spectral efficiency. So the tradeoff between the error rate and the bandwidth usage is required. The result shown is implemented at FTN factor $(\alpha) = 0.87$. The lower roll-off factors are preferred at the point of acceptable error performance. This provides an analysis for the acceptability of the FTN systems under the limitation of the error performance at given FTN rate and varying roll-off factors.

Figure 5.3 depicts the way how the FTN affects the error performance. As shown, the error rate increases with the decrease in the time period i.e., the new time period introduced by the FTN signaling αt, where $\alpha < 1$ shows how the decrease in time factor affects the result. The FTN response using MMSE equalizer for the different values of α at $1, 0.87$ and 0.75 is shown. For lower value of α, the time period of signal transmission decreases creating an environment for higher data rate but at the same time more error has to be faced.

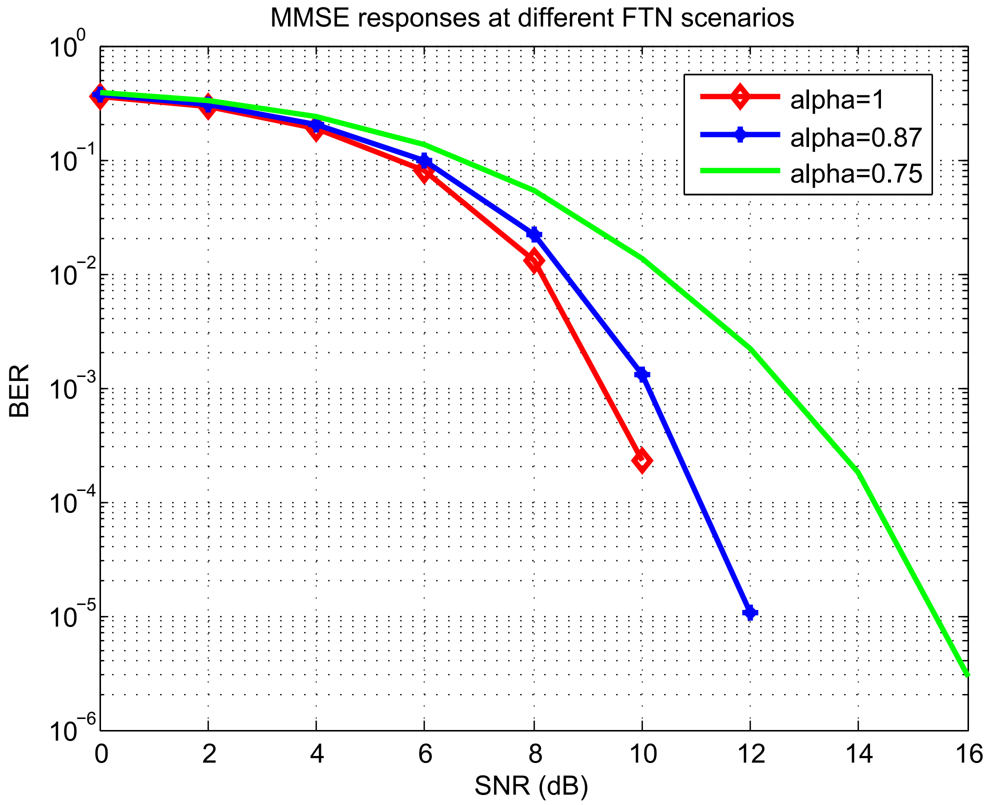

Figure 5.3: MMSE response of FTN signals at different α values.

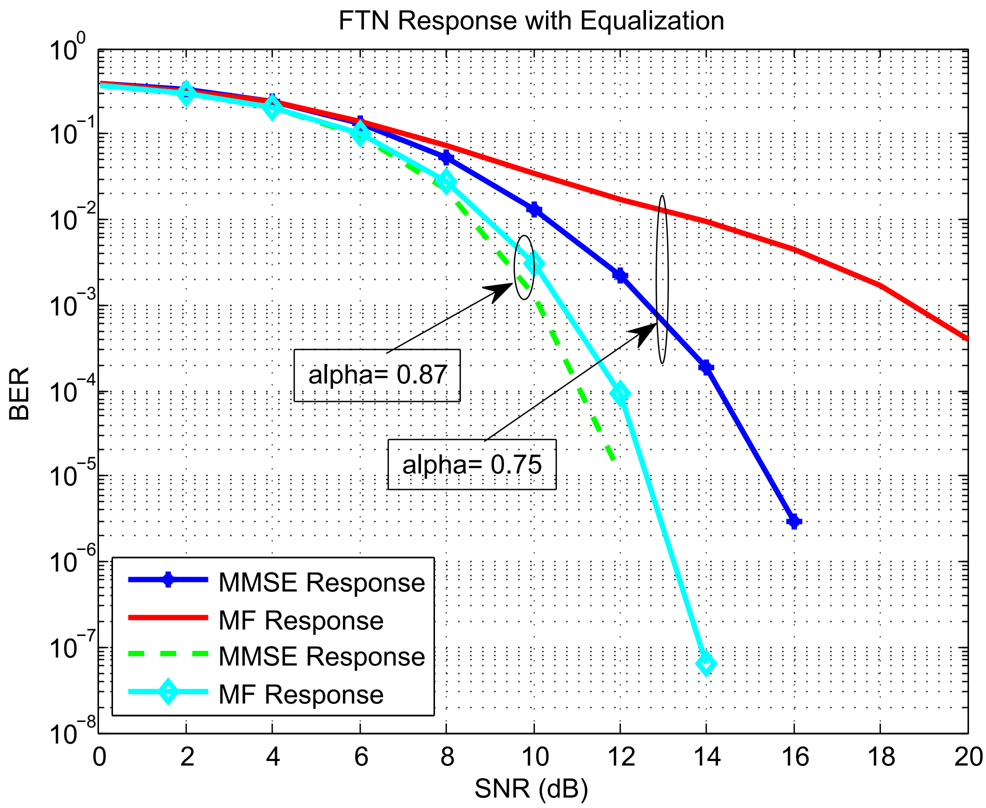

Figure 5.4: Comparative analysis of MMSE and MF response of FTN signals.

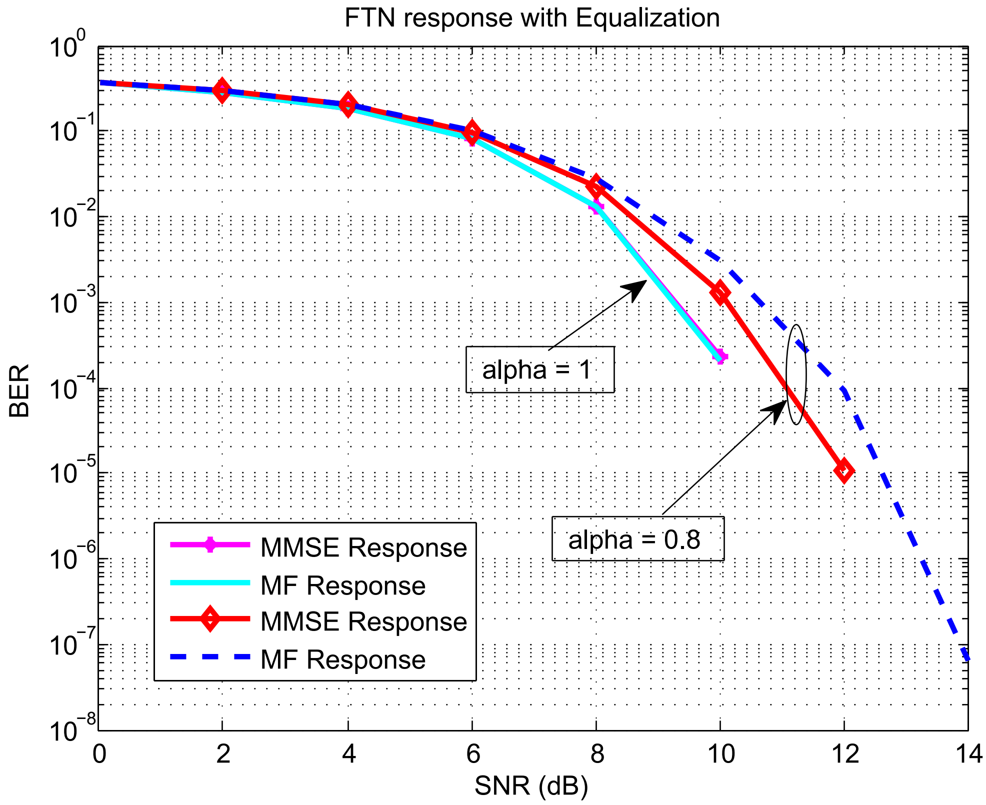

Figure 5.5: Comparative analysis of MMSE and MF response of FTN signals.

Varying the time period or the symbol packing ratio (FTN factor), the variation in the signal response is observed. The comparative high error rate for less time period is due to the generation of ISI. Lesser the time factor, more is the error. This is due to the increment of the non orthogonality behavior of the signals. The different approaches for FTN at $\alpha = 1, 0.87$ and 0.75 is shown. Figure 5.4 shows the comparative analysis of MMSE equalizer response and matched filter response at $\alpha = 0.87$ and 0.75. Likewise, Figure 5.5 shows the response at $\alpha = 1$ and 0.87. Equalizer effect is more significant for the system with reduced time period since the ISI is more notable in such case.

5.2. FTN analysis under Turbo coded system

In the thesis work, turbo code implementation is performed as the next approach to analyze the performance measure under the coded system. The binary modulated signals are encoded with the turbo encoder. Evaluation of turbo codes is measured in terms of BER. AWGN channel model is used for simplicity. Decoder performs iterative processing to ensure the acceptable error performance. Though the increase in the number of iterations improve the turbo code performance but after certain point no any significant improvement is observed thereby showing similar BER. So the iteration loop is fixed such that extra computational load is avoided. In the simulation, with BCJR decoding algorithm, it is observed that the BER decreases after each iteration, however after the fourth iteration, no further improvement is seen. The time requirement for the processing increases with the increase in the number of bits as it involves the significant increase in the number of trellis calculations.

The FTN measure for the system under this coded system is viewed after the extraction of the decoded symbols and comparing it with the original transmitted signals. BER analysis is used for the performance measurement. The results thus showed an improvement in the received signals due to the introduction of coded systems.

5.2.1. Results

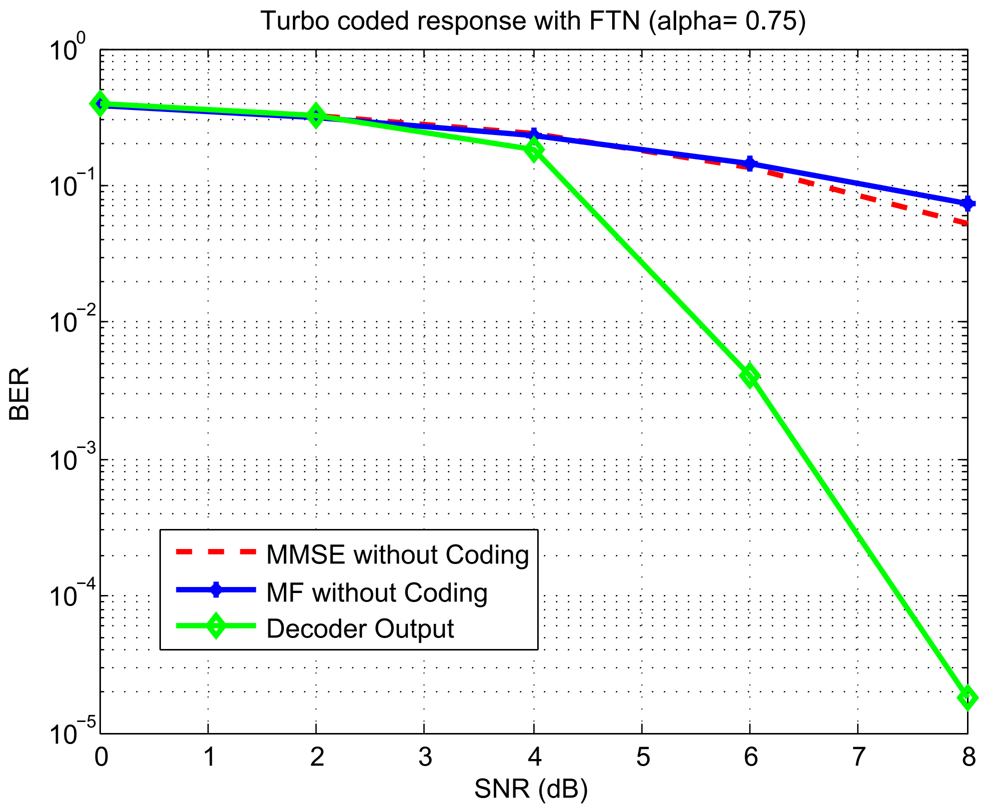

Figure 5.6: MMSE Equalization and Turbo decoding response of FTN signals.

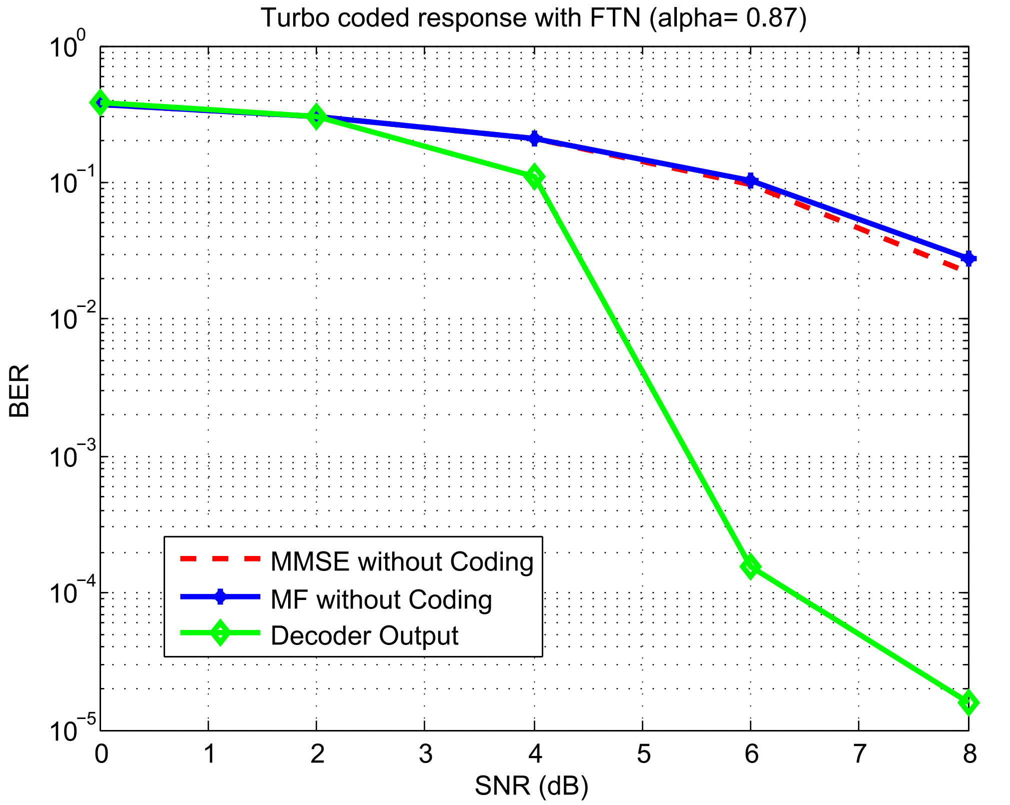

Figure 5.7: MMSE Equalization and Turbo decoding response of FTN signals.

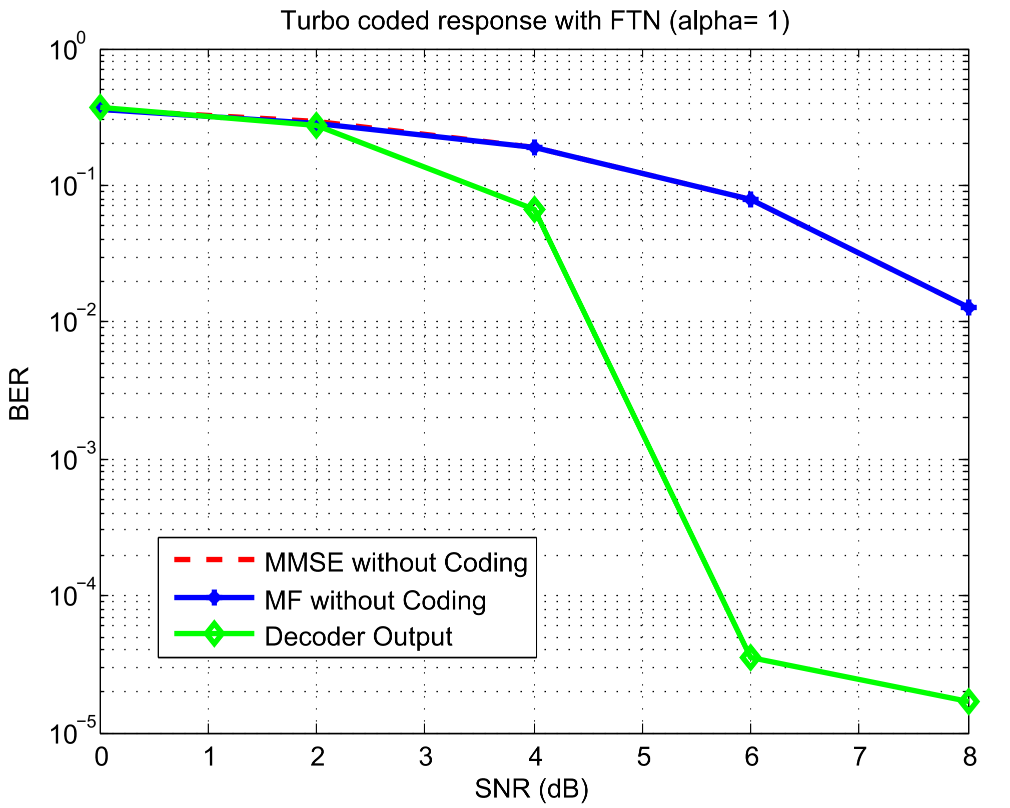

Figure 5.8: MMSE Equalization and Turbo decoding response of FTN signals.

The Figures 5.6, 5.7 and 5.8 demonstrate the comparative study of the simulated results for MF, equalizer output and the decoded results at $\alpha = 0.75, 0, 87$ and 1 respectively. The simulations are performed keeping the roll-off factor equal to 0.4 and the individual results for different FTN time factors are demonstrated. The increase in error rate for corresponding decrease in symbol duration is due to the non orthogonal signals, hence more interferences. For less time period, this non orthogonality behaviour of the transmitting signals are comparatively higher thereby creating more interferences. Equalizers are responsible for mitigating the ISI effect. The decoder are used such that they can correct the errors in the equalized symbol sequences. Turbo code implementation is carried out for lower SNR values compared to previous comparison of equalizer result at higher SNRs as they show good BER effects with lower SNR. For high SNR, decoding results are almost optimal due to the low weight codewords.

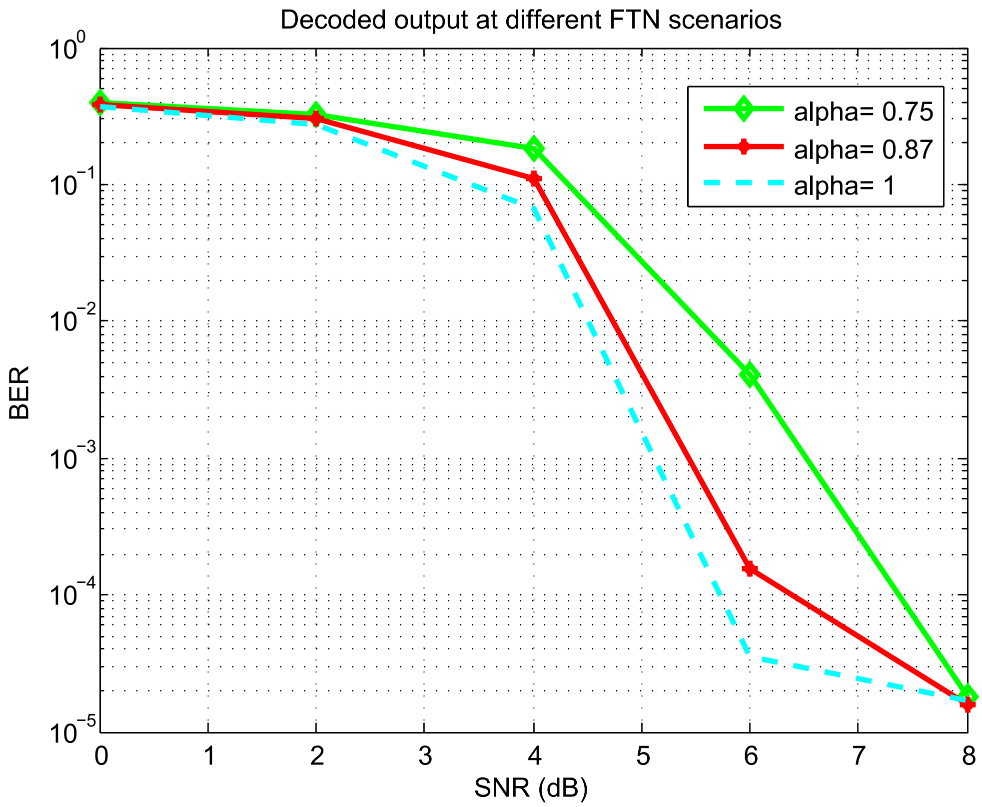

Figure 5.9: Turbo coded response for FTN signals at different α values.

Figure 5.9 shows the advantage of turbo coding output for the FTN transmitted signals. It shows the comparative analysis of the FTN signals as a decoded output at different FTN values. Results for decoded output at $\alpha = 0.75, 0, 87$ and 1 is shown. The error rate is significantly decreased at first and at the later stage it does not show distinct change for high SNR. The peculiarity seen in the graph is due to the error floor. It is seen that the BER curve falls off sharply with increasing SNR for the moderate error rates. Then the curve starts flattening at high SNR. So it is recommended to execute the BER simulation at lower values. This situation is referred as error floor. In fact this error floor inhibits the turbo code performance to achieve extremely low error rates. The low weight code words are responsible for this error floor [62]. The situation is more significant in high order SNRs.

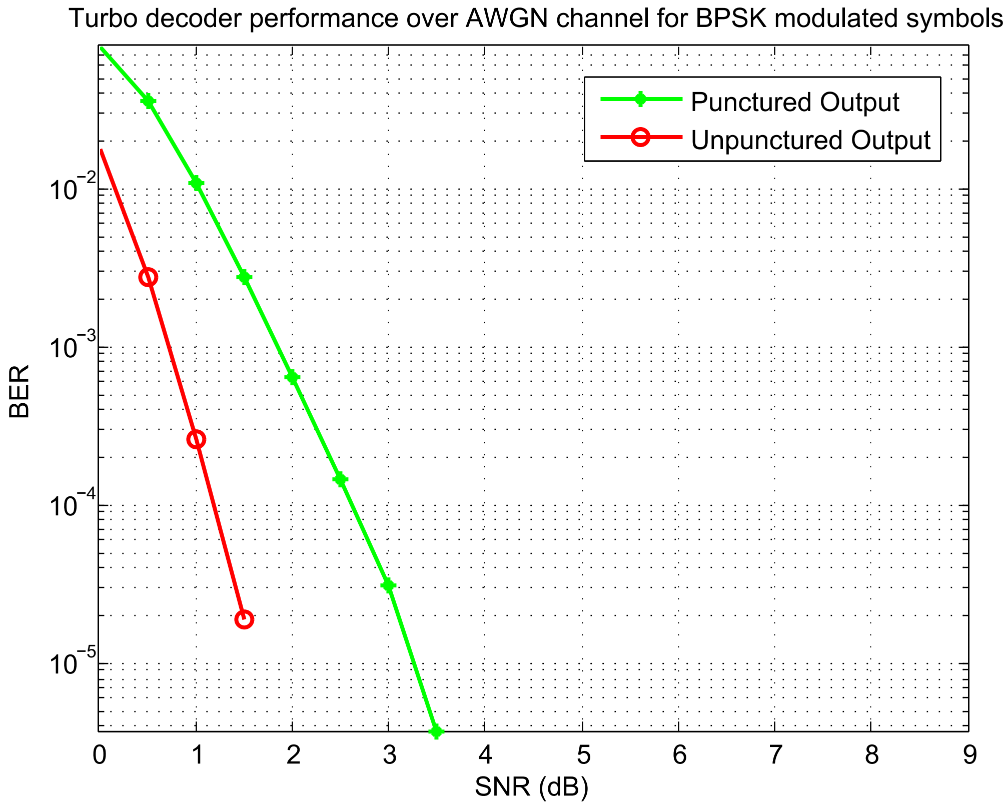

Figure 5.10: Comparative responses for Punctured and Unpunctured Turbo codes.

Simulated plots for the turbo encoded and iteratively decoded with BCJR decoding algorithm is presented in Figure 5.10. It contains the plots with code rates $1/3$ and $4/9$. At first the plot for code rate $1/3$ is generated. Then, the code is punctured to change the code rate. Using the puncturing matrix as shown in section 4.1.3 the code rate is changed to $4/9$. Puncturing increases the code rate as it allows the information to be transmitted with comparatively less number of bits than unpunctured code but at the same time BER is increased due to the reduction in the number of parity bits.

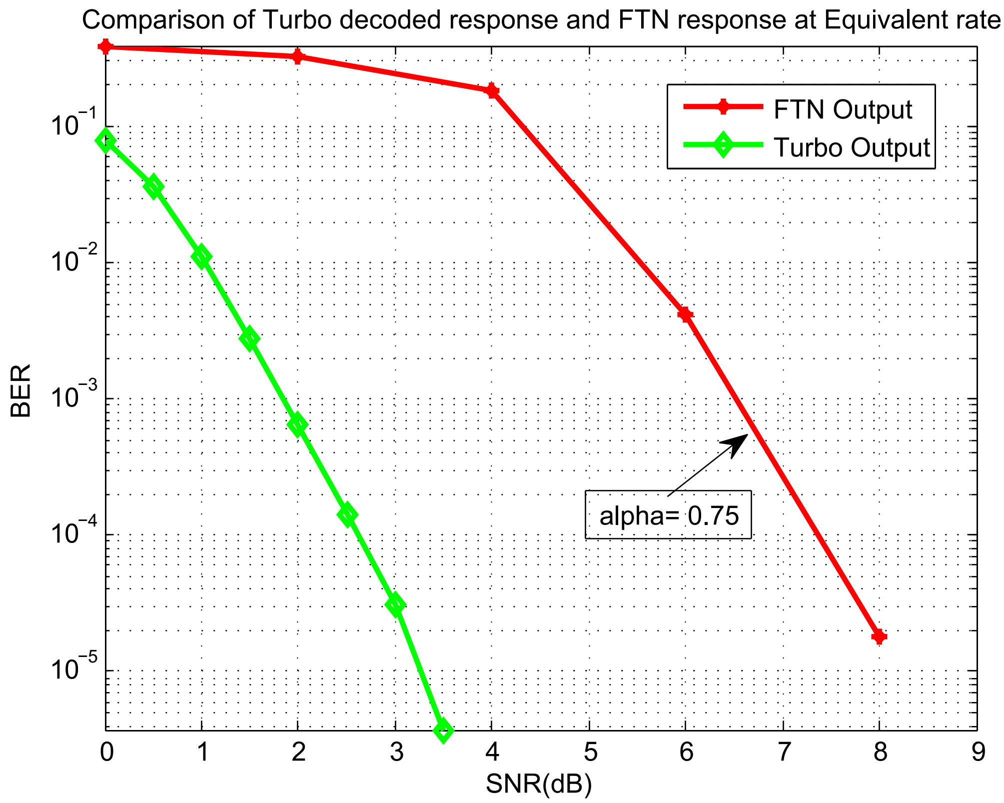

Figure 5.11: Comparative analysis making the rate equivalent for FTN and Turbo coding.

For the comparative study of FTN transmission under coding systems, the comparison is made at equivalent scenario for the rate. In Figure 5.11, first the turbo code with code rate $4/9$ is drawn. This is done by puncturing the $1/3$ code rate with puncturing matrix. This is carried out with FTN rate 1. For the next result the turbo code of rate $1/3$ and the FTN rate $8/6$ is processed to view the result. Then the comparison of the system due to this coded response with the uncoded system is justified as the overall condition provided a fair comparison for both the cases with same rate $4/9$. The result for two approaches is presented in the graph which showed that the FTN benefits come at the cost of increased error rate.

6. DISCUSSION AND FUTURE SCOPE

Considering the limited bandwidth resources availability for the future wireless communications systems, the thesis work is focused to address the issue by discussing an idea to attain high data rates without decreasing the spectral efficiency. The noble approach to use the non orthogonal pulses to reduce the symbol duration such that more data are transmitted at the given time with same spectral efficiency and error rate performance as that of orthogonal transmission systems is considered as the FTN systems.

Extending the traditional Nyquist transmission criteria for ISI free scenario to the new approach of faster data speed attainment is explored. The FTN process was introduced by modulating the pulses faster than the Nyquist rate. Taking into account of the Mazo [3] explanation of FTN signaling for the Sinc pulses, further modification is carried out. In Mazo [3], it is explained that using binary antipodal modulation, the increment in the modulation rate by 25% has no effect on the minimum euclidean distance between the closest signals. This stipulates the fact that the FTN induced transmission systems helps to increase the transmission speed without increasing bandwidth consumption. In short, it increases the bit rate and preserves the signal bandwidth. However, producing the ISI as a consequence builds an additional burden at the receiver processing. The ways to deal with this ISI is evaluated for both the coded and uncoded systems.

FTN transmission is dedicated to build an approach to transmit maximum data utilizing the minimum bandwidth possible such that it can be ensured that larger number of subscribers are possible within the given constraints. Thesis task is scrutinized for two different approaches. The coded and uncoded data bits are used for signal transmission separately and the results were investigated. System design included turbo coding systems to encode the data before modulation are given the appropriate pulse shaping. Modulation helps to improve the system performance by matching the information signal characteristics to those of the channel characteristics. Relevant selection of shaping filters and roll-off factors also showed great impact on the received signal accuracy. With the decrease in the value of roll-off factor, the spectral efficiency of the RRC pulses decrease monotonically [63]. Regarding the use of turbo encoder, the interleaver pattern and the concatenation pattern of the RSC encoders play an important role for increasing the efficiency. Using the puncturing techniques, code rate was changed and the comparison of the FTN coded and uncoded systems were made making the total rates equivalent for both the systems.

Thesis provides an approach to simplify the receiver processing techniques. Major issue comes to balance between throughput and complexity. Advantage of the FTN is discussed regarding this matter. The PSD is fixed but bit density in bits/Hz-s is higher than traditional Nyquist signaling. Since it can be inferred that the main task of FTN complexity lies at the receiver end to tackle the demodulating complexity, FTN can be the suitable approach for the uplink of a cellular network where the complexity is more at the base stations. This builds an approach to serve the high-end devices like smart phones, smart vehicles etc., in downlink. Since FTN can provide more data density without increasing signal power, they can also be a good approach for future satellite and mobile communication systems.

Thesis highlights the system that combines equalization with coded modulation. Matching the transmitter and receiver filters provide the optimum BER performance. MMSE equalizer is used to overcome the ISI and also the colored noise due to FTN.

Turbo codes are considered as a high performance error correcting codes close to Shannon limit. Statistical measures like posteriori probability and likelihood were studied to analyze the error performance with BCJR decoding algorithm. Using an iterative decoding process to these soft output, performance is improved. Thus the frequency domain equalization of the MMSE equalizer and the iterative decoding algorithm of the turbo decoder are implemented to achieve the explicit benefit eliminating the interferences. The simulation result proposes the benefits of using FTN system with low complexity receiver and better BER proficiency over conventional Nyquist transmission systems.

6.0.2. Future Studies

More powerful codes can be used to increase the throughput with the benefit of coding gains and also the optimization of the pulse signals used can be a better approach to improve the performance [64]. Moreover, higher order modulation and their effect regarding distortion sensitivity and error rate, throughput, complexity etc., on FTN system is an interesting topic [65]. Study can be further extended to improve the capacity of the system in the bandwidth starved scenario. FTN researches has led to the achievement of higher Shannon capacity and creating new capacity attributes [6]. FTN implementation in the OFDM systems and also the research over filter bank multicarrier (FBMC) is another interesting topic which is expected to overrule the existing advantages of the contemporary systems. The combination of FTN and MIMO techniques can be considered to generate new interest areas for future wireless communications. The peak average power ratio (PAPR) evaluation of FTN and the possible ways to overcome it can make it an interesting research field.

Due to the complicated receiver structure, it might be considered as a complex means to be used in future networks. However, with the improvements in receiver processing complications, this approach of FTN signaling can be forwarded as a good alternative to address the issue of high speed transmission requirement.

7. SUMMARY

The thesis work involves the study of the signal transmission and its effect when the transmission procedures are carried out going beyond the Nyquist ISI criteria. Signals are transmitted at the rate faster than the signaling rate recommended by Nyquist criteria and the results under these circumstances are scrutinized.

The FTN scheme is used as a modification over the ordinary linear modulation thereby creating a scenario where higher data rates are achieved. The receiver processing techniques explained in the thesis work makes this practically realizable. Performance results for both the coded and the uncoded systems prove the improvement over this ordinary modulation technique compared over the identical situation of bit energy, spectrum and error rate. The proposed scheme for the receiver designing with the FDE based MMSE equalizer and the iterative decoding of the received data bits with the turbo coding approach is presented. This simplifies the receiver decoding complexity. The iterative decoding used in the turbo decoder structure showed the comparative improvement in the system performance. Simulation results highlight the advantage of FTN implementation in the signal transmission process. Error rate of an orthogonal transmission system is achieved nearly even with the non orthogonal signal usage. To achieve the more data rate for the given bit energy, and the error rate, the FTN signals makes use of the excess pulse bandwidth for the signal transmission which ultimately ends up in less bandwidth consumption. This created an opportunity that more symbols could be transmitted at the given time period. FTN implementation is therefore the promising approach to help achieve the higher data rates at the cost of same bandwidth consumption, bit energy and error rate as that of Nyquist transmission. In FTN, the signals are no longer orthogonal with respect to symbol time. Using the non orthogonal pulses as the pulse signal is the key aspect to improve the speed. FTN factor represents the speed factor. Different FTN factors yield different results. Less the value of this FTN factor, higher is the speed of transmission. This is viewed from frequency domain aspect as the squeezing of the more signals together. The ISI which acts as a dominant limiting factor, occurred due to such non orthogonal pulses are minimized with the use of MMSE equalization method and the iterative approach of BCJR decoding algorithm.

The analysis of the simulation results for both coded and uncoded signal transmission schemes emphasize the importance of FTN signaling to be used in the future wireless communication systems.

BIBLIOGRAPHY

[1] El Hefnawy M. & Taoka H. (2013) Overview of Faster-than-Nyquist for future mobile communication systems. In: *Vehicular Technology Conference (VTC Spring), 2013 IEEE 77th*, IEEE, pp. 1–5.

[2] Proakis J.G. (1995) Digital communications. New York ; Singapore : McGraw-Hill, third edition.

[3] Mazo J. (1975) Faster-than-Nyquist signaling. The Bell System Technical Journal 54, pp. 1451–1462.

[4] Rusek F. & Anderson J.B. (2008) Non binary and precoded faster than Nyquist signaling. IEEE Transactions on Communications 56, pp. 808–817.

[5] Sugiura S. (2013) Frequency-Domain Equalization of Faster-than-Nyquist Signaling .

[6] Anderson J.B., Rusek F. & Owall V. (2013) Faster-than-Nyquist signaling. Proceedings of the IEEE 101, pp. 1817–1830.

[7] Tomoki S. & Adachi F. (2003) Comparative study of various frequency equalization techniques for downlink of a wireless OFDM-CDMA system. IEICE transactions on communications 86, pp. 352–364.

[8] Berrou C., Glavieux A. & Thitimajshima P. (May 1993) Near Shannon limit error-correcting coding and decoding: Turbo-codes.1,. In: *Technical Program, Conference Record, IEEE International Conference on Communications, ICC '93 Geneva,*, volume 2, pp. 1064–1070.

[9] Decoding S.I. (2005) Transactions Letters. IEEE Transactions on Communications 53, pp. 209.

[10] Divsalar D. & Pollara F. (1995) Multiple turbo codes for deep-space communications .

[11] Patel S., Chauhan M. & Kapadiya K. (2012) 5G: Future mobile technology-vision 2020. International Journal of Computer Applications 54.

[12] Monserrat J.F., Droste H., Bulakci O., Eichinger J., Queseth O., Stamatelatos M., Tullberg H., Venkatkumar V., Zimmermann G., Dotsch U. et al. (2014) Rethinking the mobile and wireless network architecture: The METIS research into 5G. In: *European Conference on Networks and Communications (EuCNC), 2014*, IEEE, pp. 1–5.

[13] Sharma P. (2013) Evolution of mobile wireless communication networks-1G to 5G as well as future prospective of next generation communication network. International Journal of Computer Science and Mobile Computing 2, pp. 47–53.

[14] Li Q., Niu H., Papathanassiou A. & Wu G. (2014) 5G network capacity: Key elements and technologies. Vehicular Technology Magazine, IEEE 9, pp. 71–78.

[15] Haider F., Gao X., You X.H., Yang Y., Yuan D., Aggoune H.M. & Haas H. (2014) Cellular architecture and key technologies for 5G wireless communication networks. IEEE Communications Magazine p. 123.

[16] Tudzarov A. & Janevski T. (2011) Functional architecture for 5G mobile networks. International Journal of Advanced Science and Technology 32, pp. 65–78.

[17] Patil S., Patil V. & Bhat P. (2012) A review on 5G technology. International Journal of Engineering and Innovative Technology (IJEIT) 1, pp. 26–30.

[18] Osseiran A., Boccardi F., Braun V., Kusume K., Marsch P., Maternia M., Queseth O., Schellmann M., Schotten H., Taoka H. et al. (2014) Scenarios for 5G mobile and wireless communications: the vision of the METIS project. IEEE Communications Magazine 52, pp. 26–35.

[19] Soldani D. & Manzalini A. (2014) A 5G Infrastructure for Anything-as-a-Service. Journal of Telecommunications System & Management pp. 2167–0919.

[20] Sapakal M.R.S. & Kadam M.S.S. (2013) 5G Mobile Technology. International Journal of Advanced Research in Computer Engineering & Technology 2.

[21] Huawei (2013) A 5G technology vision. Technical report, Huawei Technologies Co., Ltd.

[22] Nyquist H. (1928) Abridgment of certain topics in telegraph transmission theory. Journal of the AIEE, 47, pp. 214–217.

[23] Oshana R. (2006) DSP Software Development Techniques for Embedded and Real-Time Systems. Embedded Technology, Elsevier Science.

[24] Nyquist H. (1928) Certain topics in telegraph transmission theory. Transactions of the American Institute of Electrical Engineers, 47, pp. 617–644.

[25] Kang A. & Sharma V. (2011) Pulse Shape Filtering in Wireless Communication-A Critical Analysis. Pulse 2.

[26] KavehPahlavan A.H.L. (2005) Wireless Information Networks. In: *Wireless Information Networks*, John Wiley and Sons.

[27] Wu Z., Zhu F. & Nassar C.R. (2002) Ultra wideband time hopping systems: performance and throughput enhancement via frequency domain processing. In: *Conference Record of the Thirty-Sixth Asilomar Conference on Signals, Systems and Computers, 2002.*, IEEE, volume 1, pp. 722–727.

[28] Zeng D., Annamalai A. & Zaghloul A.I. (2003) Pulse shaping filter design in UWB system. In: *IEEE Conference on Ultra Wideband Systems and Technologies, 2003*, IEEE, pp. 66–70.

[29] Datacom P. (2012) Saving Satellite Bandwidth by Optimising Spectral Roll-off. Teledyne Paradise Datacom Application Note .

[30] Bonnaud A., Feltrin E. & Barbiero L. (2014) DVB-S2 Extension: End-to-End Impact of Sharper Roll-Off Factor Over Satellite Link. In: *The Sixth International Conference on Advances in Satellite and Space Communications, SPACOMM 2014,*, pp. 36–41.

[31] Gentile K. (2002) The care and feeding of digital, pulse-shaping filters. RF DESIGN 25, pp. 50–58.

[32] Xia X.G. (1997) A family of pulse-shaping filters with ISI-free matched and unmatched filter properties. IEEE Transactions on Communications, 45, pp. 1157–1158.

[33] Rha P.S. & Hsu S. (2003) Peak-to-average ratio (PAR) reduction by pulse shaping using a new family of generalized raised cosine filters. In: *IEEE 58th Vehicular Technology Conference, 2003. VTC 2003-Fall.*, IEEE, volume 1, pp. 706–710.

[34] Korowajczuk L. (2011) LTE, WiMAX and WLAN Network Design, Optimization and Performance Analysis. Wiley.

[35] Richardson A. (2005) WCDMA Design Handbook. Cambridge University Press.

[36] Alagha N.S. & Kabal P. (1999) Generalized raised-cosine filters. IEEE Transactions on Communications, 47, pp. 989–997.

[37] Mahafza B. (1998) Introduction to Radar Analysis. Electrical Engineering Radar Signal Processing, Taylor & Francis.

[38] Mahafza B. (2005) Radar Systems Analysis and Design Using MATLAB Second Edition. Taylor & Francis.

[39] Chitode J. (2008) Communication Systems - I. Technical Publications.

[40] Golden P., Dedieu H. & Jacobsen K. (2005) Fundamentals of DSL Technology. Taylor & Francis.

[41] F.M.J.Willems (2010), Colored Noise. University Lecture, Technische Universiteit Eindhoven.

[42] Das J. (2003) Review Of Digital Communication. New Age International (P) Limited.

[43] Fazel K. & Kaiser S. (2008) Multi-Carrier and Spread Spectrum Systems: From OFDM and MC-CDMA to LTE and WiMAX,. Wiley.

[44] Berrou C. & Glavieux A. (1996) Near optimum error correcting coding and decoding: Turbo-codes. IEEE Transactions on Communications, 44, pp. 1261–1271.

[45] Berrou Glavieux T. (1993) Near Shannon limit error-correcting coding and decoding pp. 1064–1070.

[46] M. Reza Soleymani Y. (2002) Turbo Coding for Satellite and Wireless Communications. In: *Turbo Coding for Satellite and Wireless Communications*, The Springer International Series in Engineering and Computer Science,USA, volume 702.

[47] Deshmukh R.M. & Ladhake S. (2009) Analysis of Various Puncturing Patterns and Code Rates: Turbo Code. International Journal of Electronic Engineering Research 1, pp. 79–88.

[48] Käsper E. (2010) Turbo codes. ekasper [at] tcs. hut. fi .

[49] Narayanan K.R. & Stuber G.L. (1997) A novel ARQ technique using the turbo coding principle. IEEE Communications Letters 1, pp. 49–51.

[50] Rusek F. & Anderson J.B. (2006) Serial and parallel concatenations based on faster than Nyquist signaling. In: *Information Theory, 2006 IEEE International Symposium on*, IEEE, pp. 1993–1997.

[51] Benedetto S. & Montorsi G. (1996) Unveiling turbo codes: Some results on parallel concatenated coding schemes. IEEE Transactions on Information Theory 42, pp. 409–428.

[52] Benedetto S., Garello R. & Montorsi G. (1998) A search for good convolutional codes to be used in the construction of turbo codes. IEEE Transactions on Communications 46, pp. 1101–1105.

[53] Hagenauer J., Offer E. & Papke L. (1996) Iterative decoding of binary block and convolutional codes. IEEE Transactions on Information Theory 42, pp. 429–445.

[54] Kousa M.A. & Mugaibel A. (2002) Puncturing effects on turbo codes. In: *IEE Proceedings-Communications*, IET, volume 149, pp. 132–138.

[55] Benedetto S., Divsalar D., Montorsi G. & Pollara F. (1997) A soft-input soft-output APP module for iterative decoding of concatenated codes. IEEE Communications Letters 1, pp. 22–24.

[56] Robertson P., Villebrun E. & Hoeher P. (1995) A comparison of optimal and sub-optimal MAP decoding algorithms operating in the log domain. In: *IEEE International Conference on Communications, ICC'95 Seattle,'Gateway to Globalization', 1995*, IEEE, volume 2, pp. 1009–1013.

[57] Valenti M.C. (2004), Turbo codes- Decoding and Applications. University Lecture, CITR, West Virginia University.

[58] Robertson P. & Worz T. (1996) A novel bandwidth efficient coding scheme employing turbo codes. In: *IEEE International Conference on Communications, ICC'96, Conference Record, Converging Technologies for Tomorrow's Applications. 1996*, IEEE, volume 2, pp. 962–967.

[59] J. G. Proakis M.S. (2008) Digital communications. In: *Digital communications, 5th ed., McGraw- Hill, NY, 2008.*, McGraw- Hill, NY.

[60] Clark M.V. (1998) Adaptive frequency-domain equalization and diversity combining for broadband wireless communications. IEEE Journal on Selected Areas in Communications 16, pp. 1385–1395.

[61] Falconer D., Ariyavisitakul S.L., Benyamin-Seeyar A. & Eidson B. (2002) Frequency domain equalization for single-carrier broadband wireless systems,. IEEE Communications Magazine, 40, pp. 58–66.

[62] Valenti M.C. & Sun J. (2004) Turbo codes. Handbook of RF and Wireless Technologies pp. 375–400.

[63] Hefnawy M.E. & Kramer G. (2014) Impact of Spectrum Sharing on the Efficiency of Faster-Than-Nyquist Signaling. arXiv preprint arXiv:1401.7262 .

[64] Dasalukunte D., Öwall V., Rusek F. & Anderson J.B. (2014) Conclusion and Future Directions. In: *Faster than Nyquist Signaling*, Springer, pp. 129–132.

[65] (August 2013) Requirements analysis and design approaches for 5G air interface. Technical Report ICT-317669-METIS/D2.1, Mobile and wireless communications Enablers for the Twenty-twenty Information Society.